Hydrogen Generation by Cold Fusion Process in Hydro Machinery

Farzan Amini

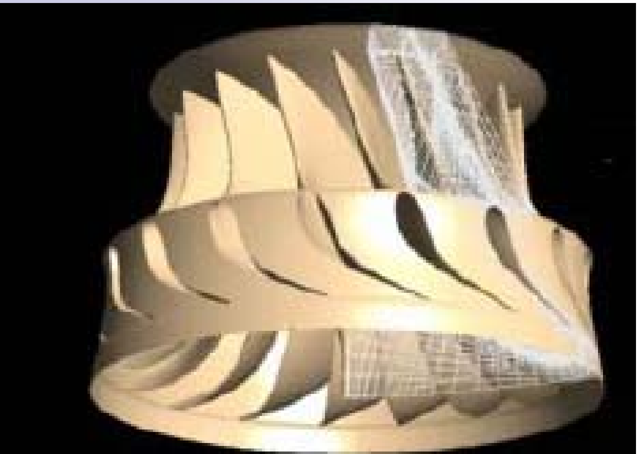

8th International workshop on Anomalies in Hydrogen/Deuterium Loaded Metals

Contents

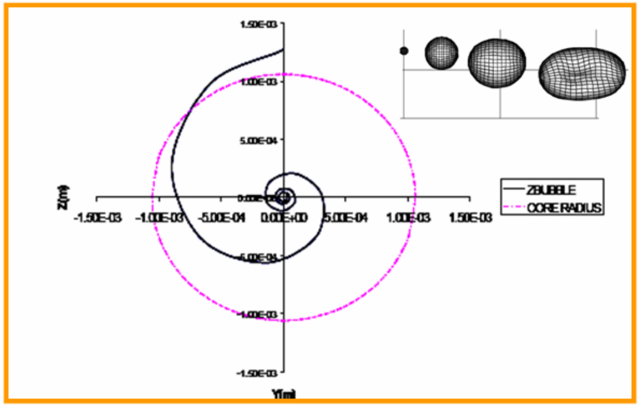

1.50E-03
1.00E-03
5.00E-04
-5.00E-04
-1.00E-03
-1.50E-03
Z(m)
-1.50E-03
-1.00E-03
-5.00E-04
0.00E+00
5.00E-04
1.00E-03
1.50E-03
Y(m)
ZBUBBLE
CORE RADIUS

1 Introduction

- Turbine Type Francis
- Turbine 255 MW
- Rotational Speed 187.5 rpm
- Runner Diameter 4.5 m

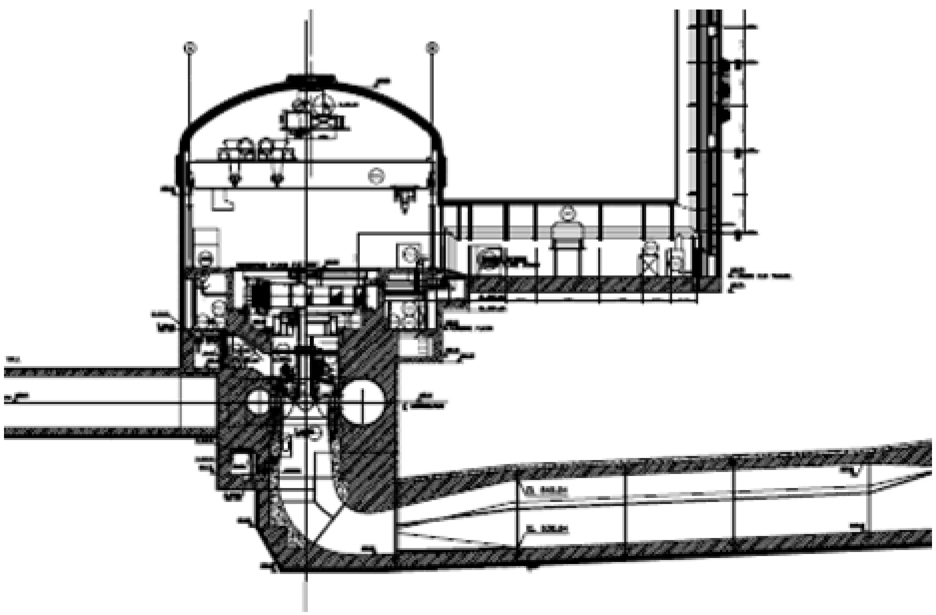

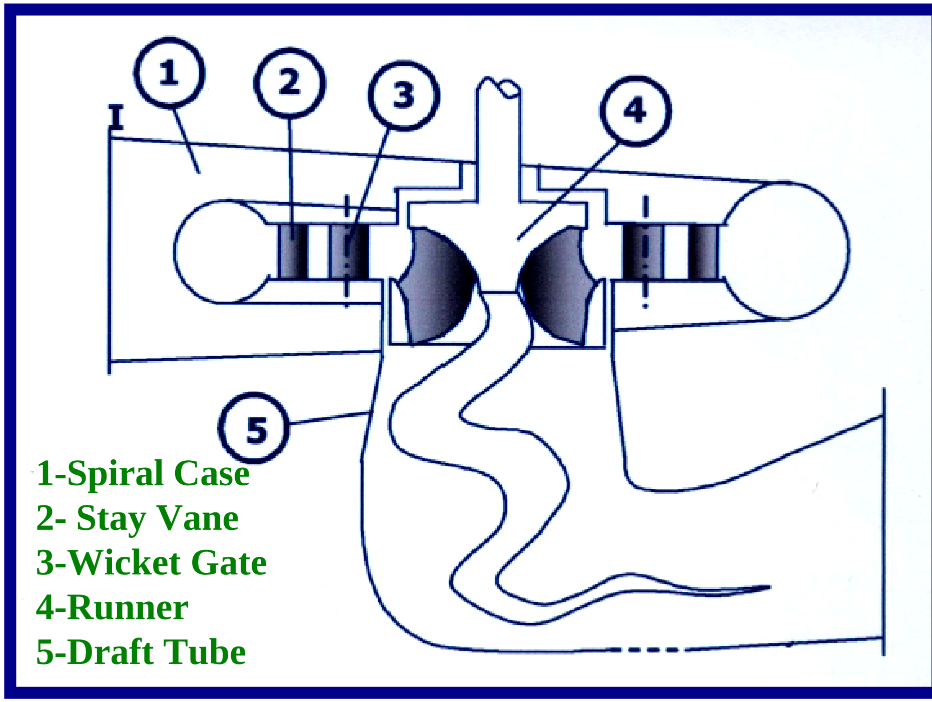

1 Introduction (cont'd)

- The operating point is determined by head and flow coefficients, defined as:

$$\psi = \frac{2E}{\omega^2 R^2} \qquad \varphi = \frac{Q}{\pi \omega R^3}$$

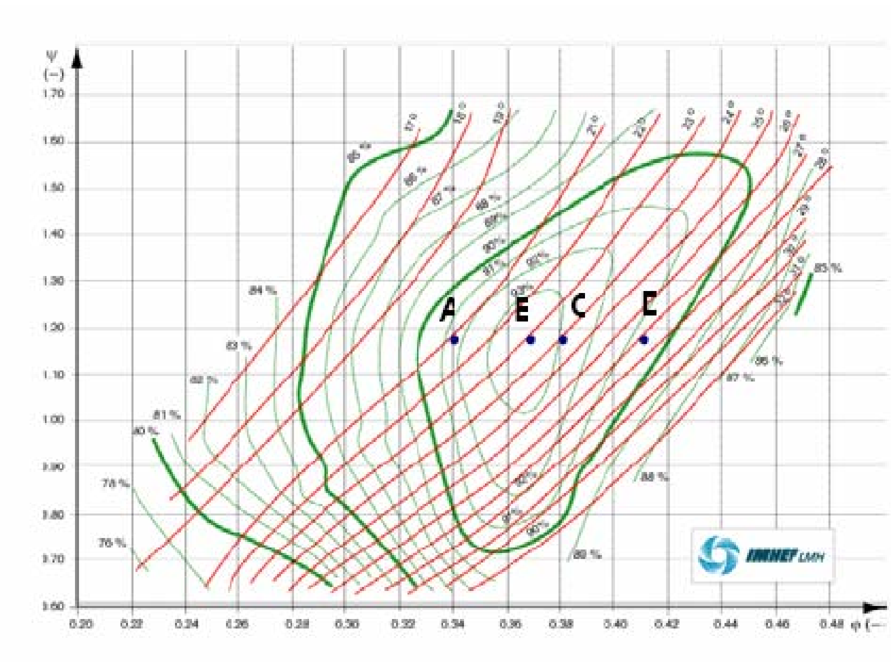

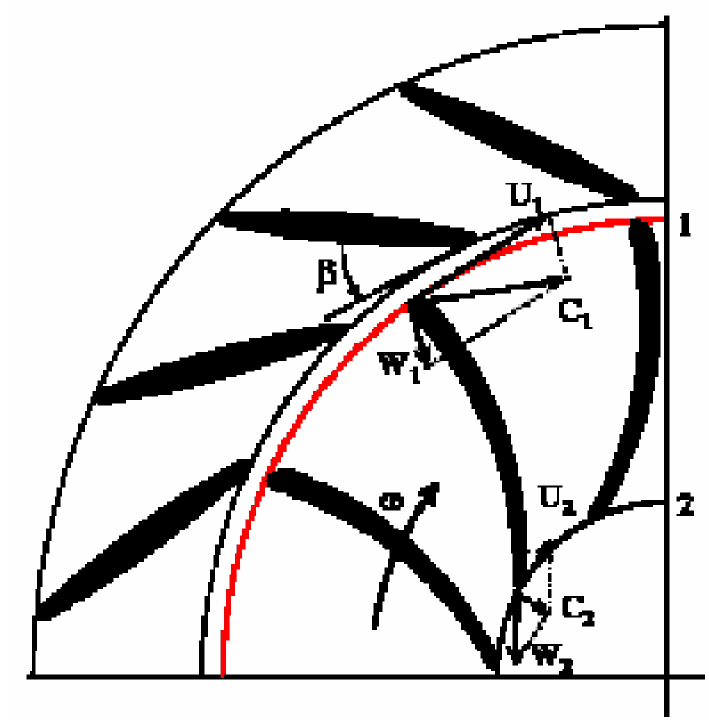

2 Bubble dynamic behavior in Hydro turbine

- Effective parameters on the bubble size
  - 2.1 Cavitation coefficient and inception
  - 2.2 Helical vortex
  - 2.3 Fission fragments
  - 2.4 pressure pulsation
  - 2.5 Resonance
  - 2.6 Effects of pressure and sound velocity

2.1 Cavitation Coefficient and inceptio...

- **Turbine Setting Level**

$$\sigma_p = \frac{NPSE}{E}$$

$$NPSE = \frac{p_I}{\rho} + g(Z_I - Z_{\text{ref}}) + \frac{1}{2}C_I^2 - \frac{p_v}{\rho}$$

$$NPSE = \frac{p_a}{\rho} - gH_S + \frac{1}{2}C_I^2 - \frac{p_v}{\rho}.$$

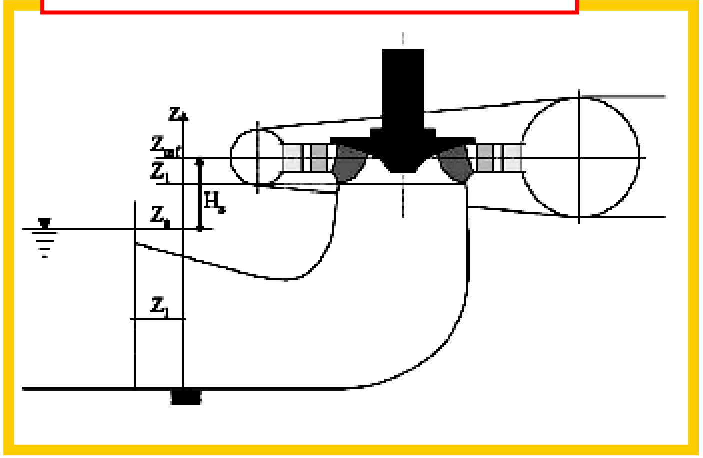

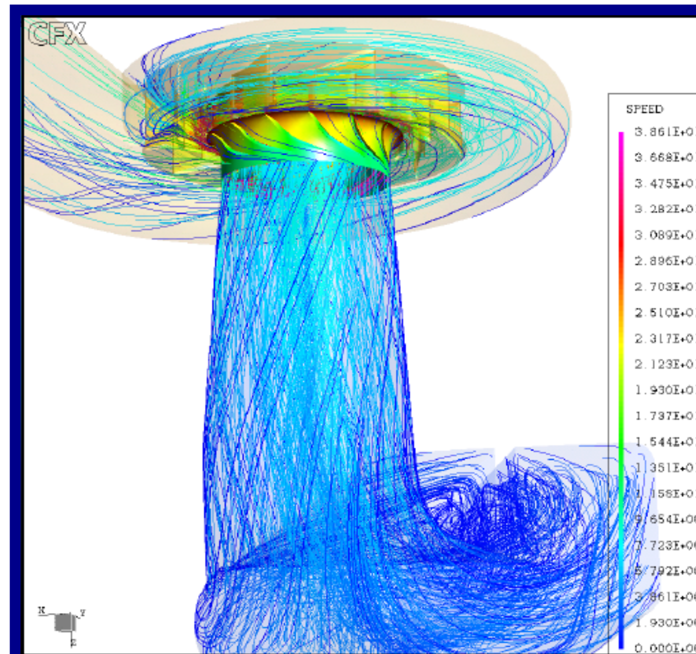

2.1Cavitation Coefficient and inception (cont'd)

- **Main Types of Cavitation**
  - Leading edge cavitation(Fig.1)
  - Traveling bubble cavitation(Fig.2)
  - Draft tube swirl(Fig.3)
  - Inter blade vortex cavitation(Fig.4)

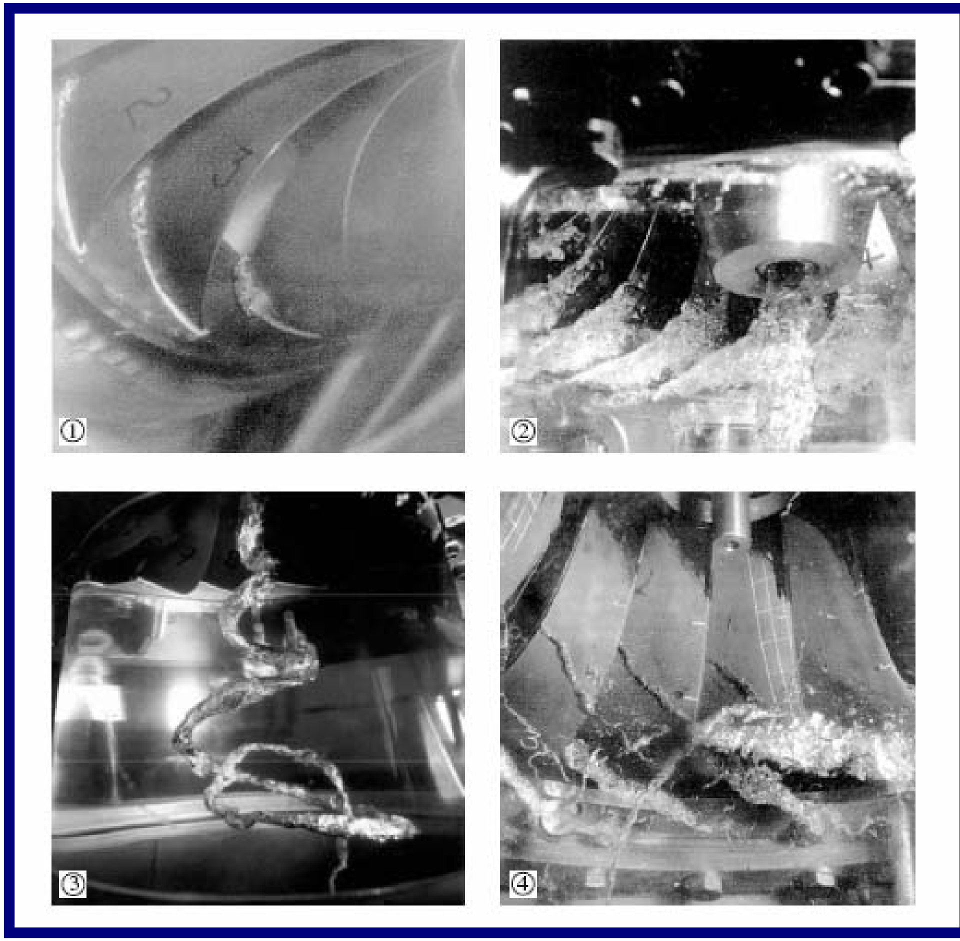

2.1 Cavitation Coefficient and inception (cont'd)

- **The pressure coefficient Cp is calculated as :Cp=(P_i-P_{REF})/H**

The pressure coefficient Cp is calculated as :Cp=(P_i-P_{REF})/H
Cp - Pressure coefficient
Pi - Pressure of each point
RREF – The pressure of the reference point, we define it with the cross point of the runner crown and the pressure side of the blade outlet. PRE
PREF = H x σ+Hv
Hv- Vapor pressure , Hv = 0.24 mH2O under - Plant cavitation factor

Comparison between pressure in the inlet and outlet of runner blade of model

				near inlet:		near outlet:	
n_{11}(rpm)	Q_{11}	σp	P_{REF} mH_2O-M	Cp	Pi-Model	Cp	Pi-Model
67.09	0.7	0.098	2.198	-0.022	1.758	-0.08	0.678

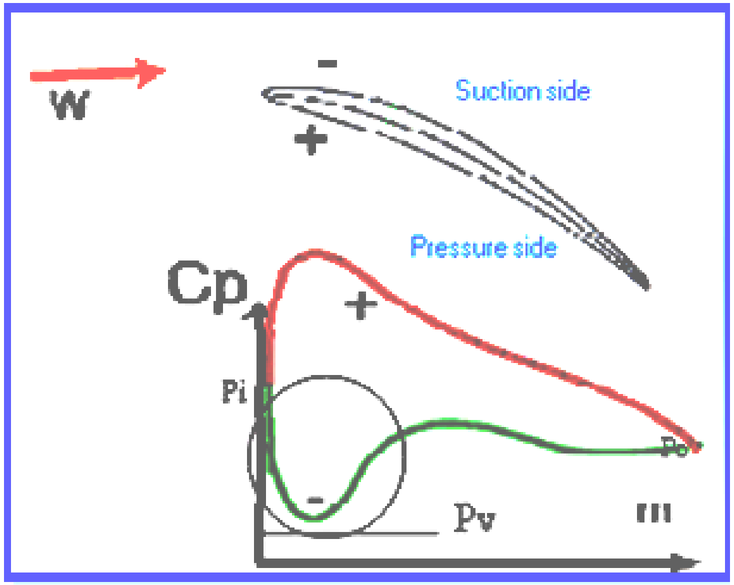

2.1 Cavitation Coefficient and inception (cont'd)

- Amplitude of pressure pulsation
- Number of bubbles
- Size of bubbles

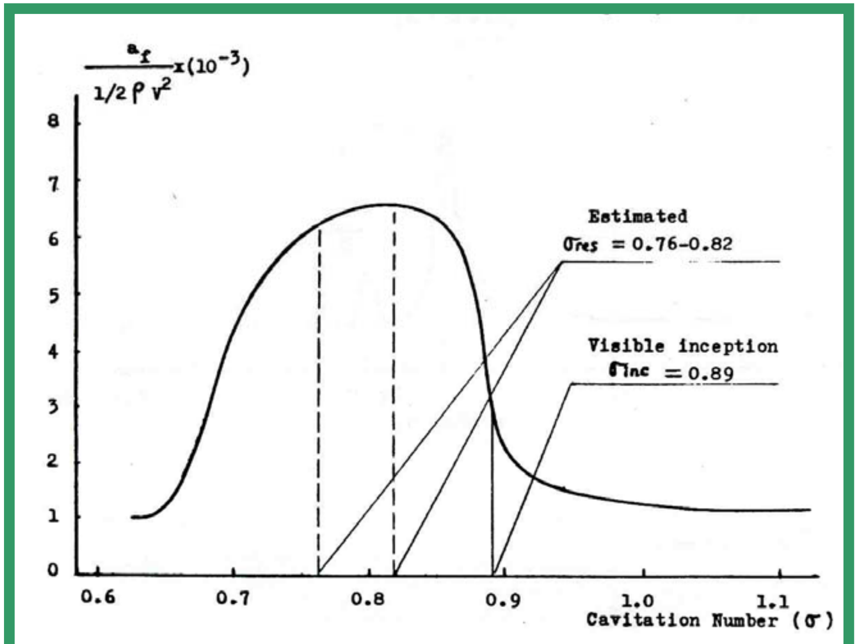

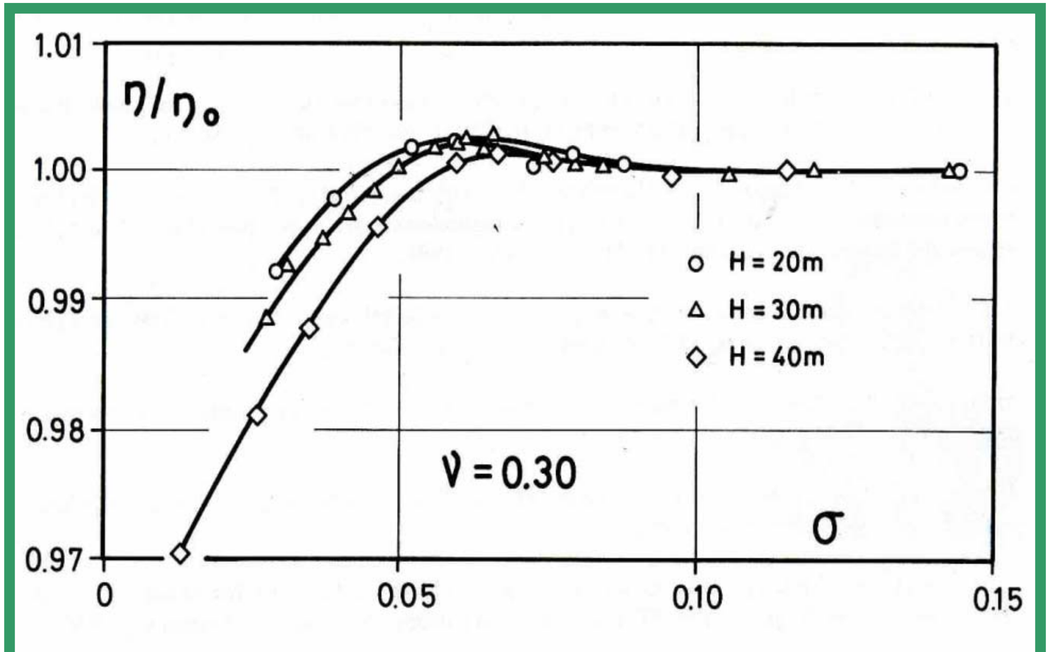

2.2 Helical Vortex

- **Operation Stability**

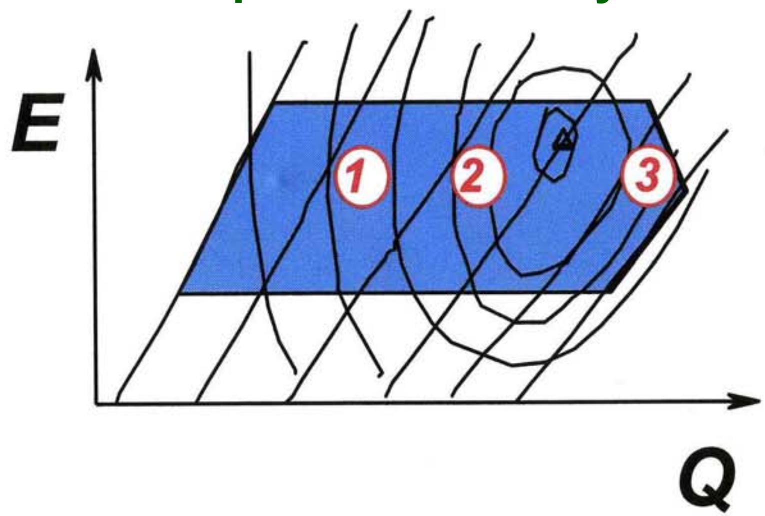

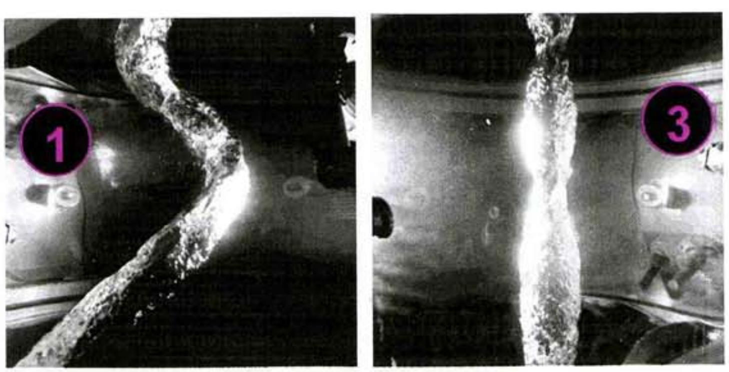

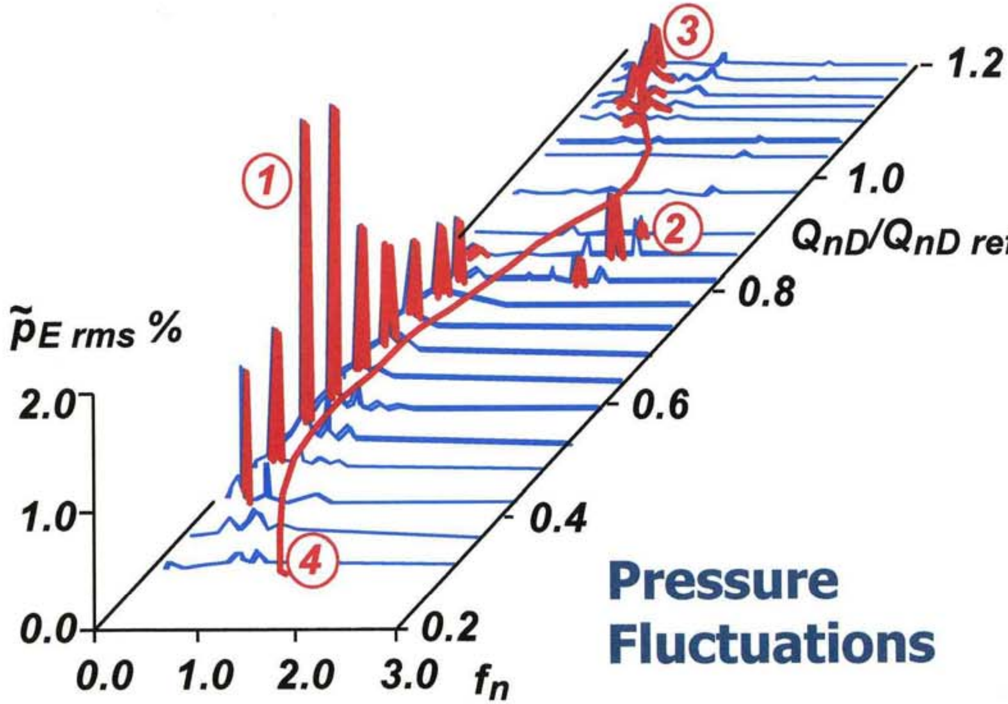

Pressure Fluctuations

2.2 Helical Vortex (cont'd)

- Size of Vortex
- Type of Vortex

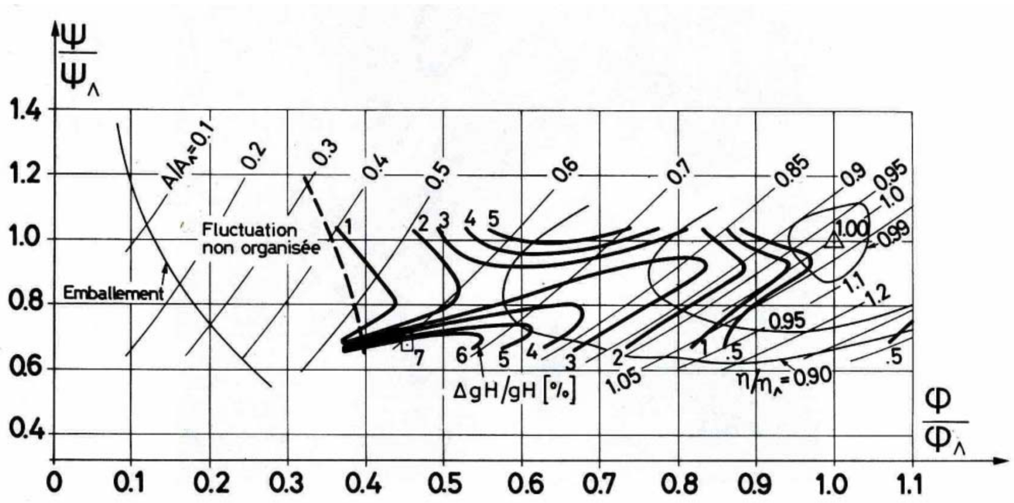

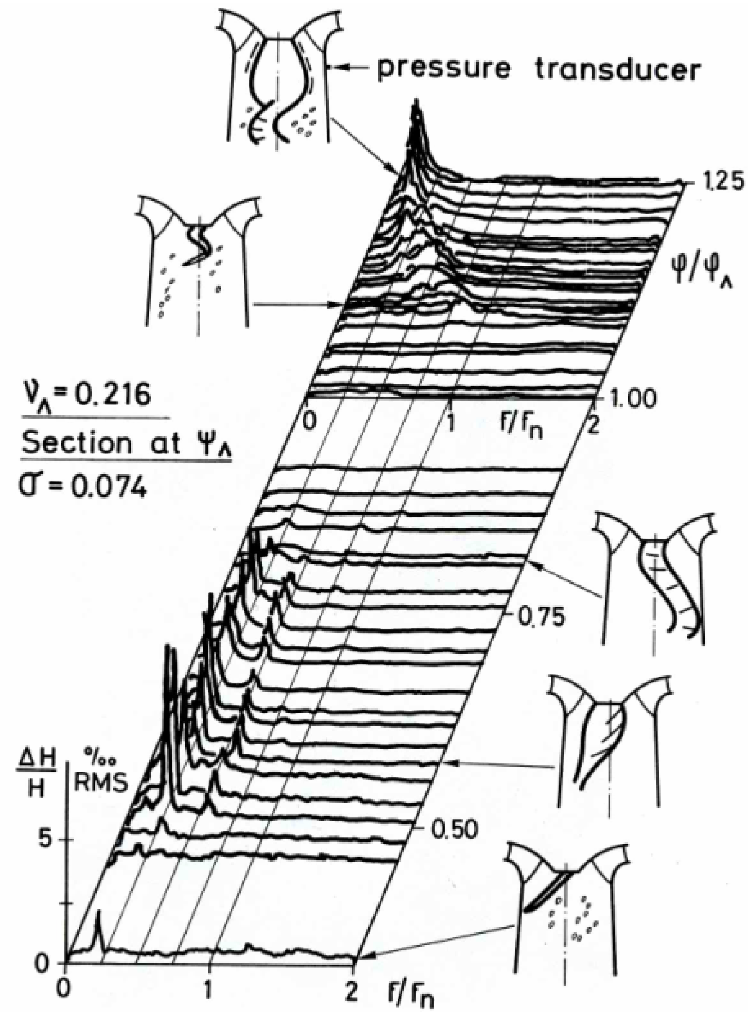

2.2 Helical Vortex (cont'd)

Draft Tube Natural Frequency

- The frequency of the draft tube excitation lies in the range of frequencies from f_E =0.786 to 1.095 Hz

$$f_0 = \frac{1}{2\pi}\sqrt{\frac{1}{\underbrace{\frac{-\partial V_c}{\partial NPSE}}_{\text{Cavitation Compliance}}\int\frac{d\ell}{A}}}$$

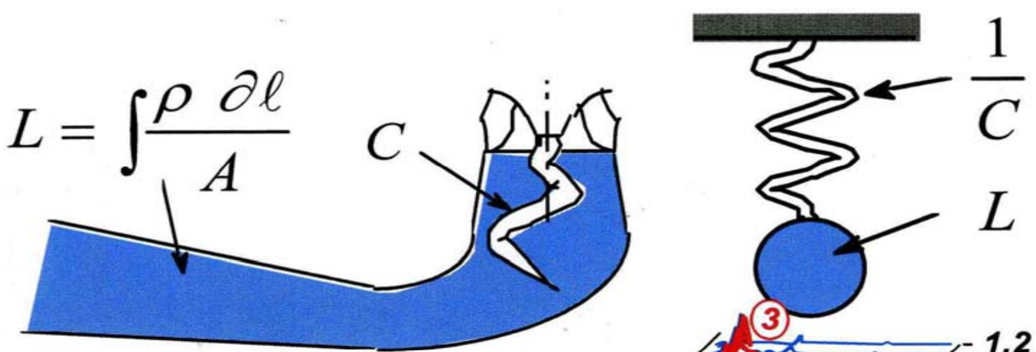

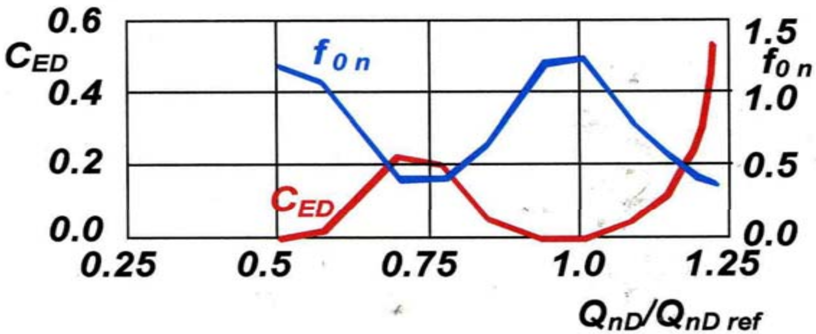

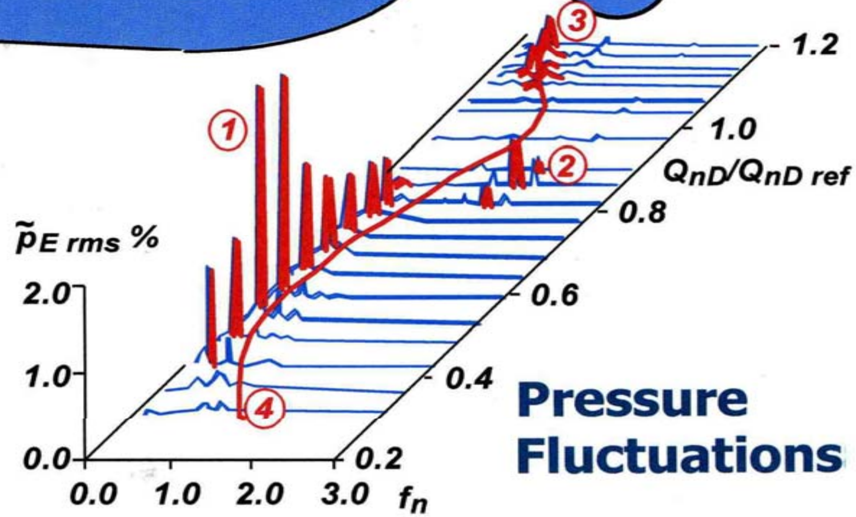

2.3 Fission Fragment

- Various values of the parameters C_Q and Cavitation number –Load Rejection Case

$$C_Q = C_P(k-1)^{\frac{1}{3}}(\alpha - 1 + \sigma)^{\frac{1}{3}}(1-\sigma)^{\frac{1}{2}}$$

$$R_o^* = \frac{R_o(p_\infty^i - p_\infty^m)}{S}$$

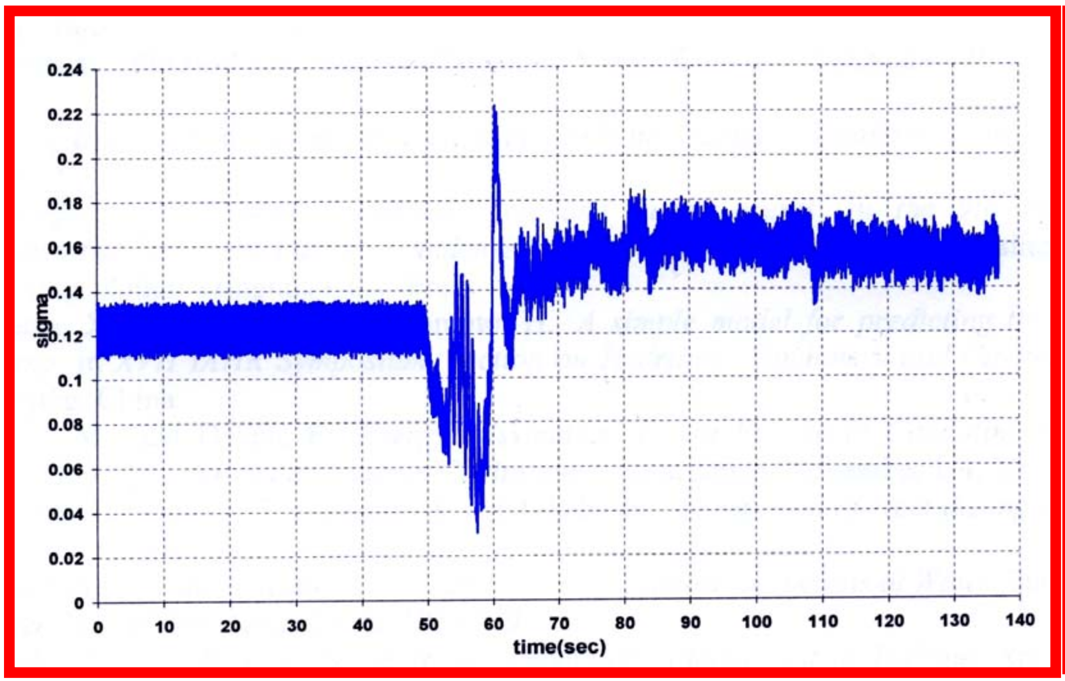

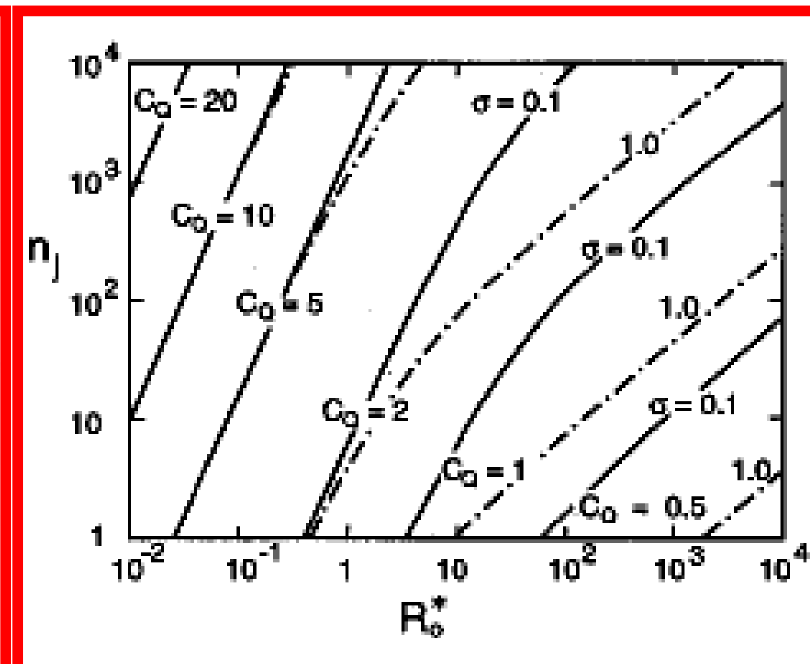

2.4 Pressure Pulsation

- Vortex region:

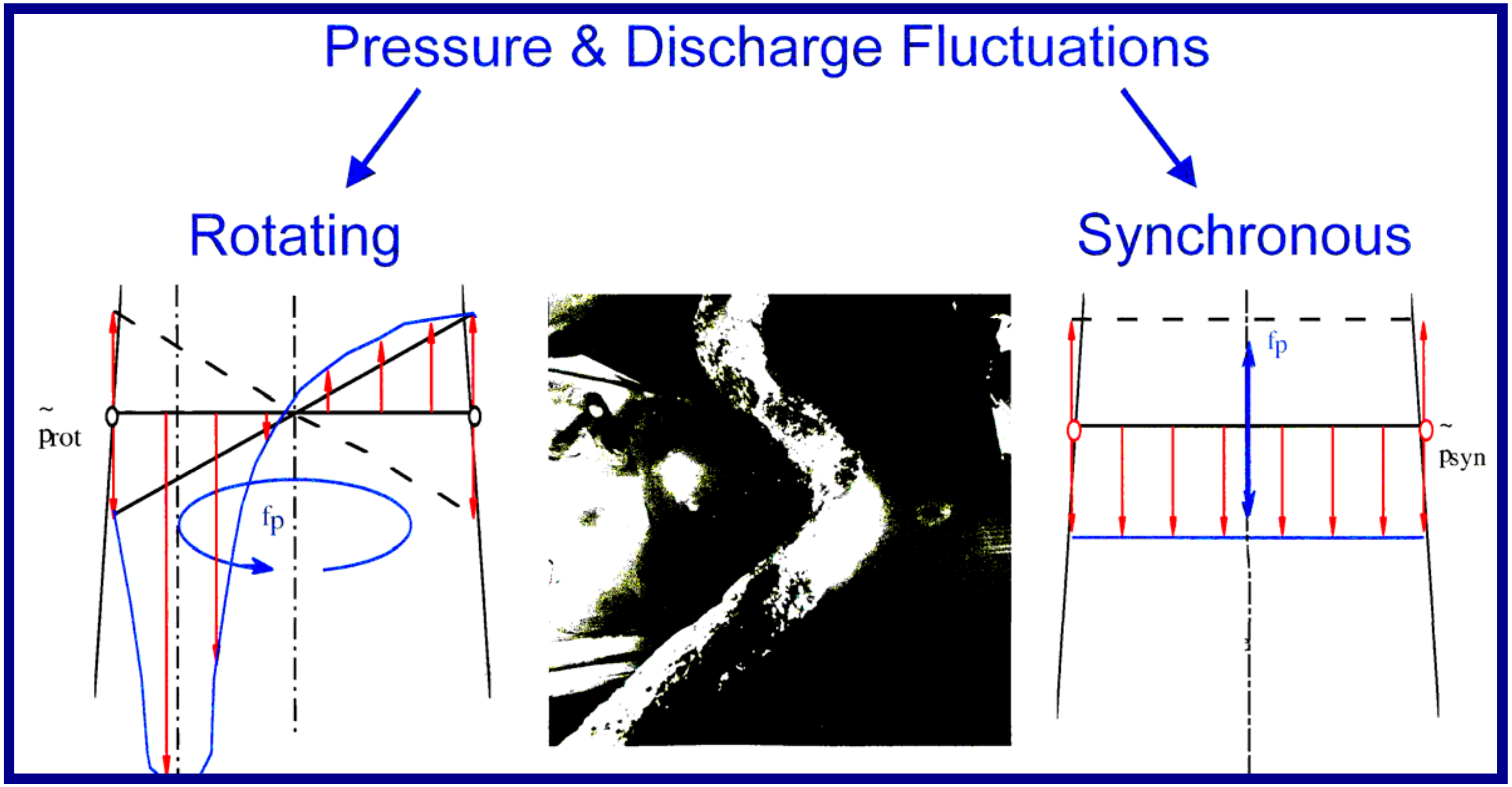

2.4 Pressure Pulsation(cont'd)

- Oscillation modes in the reaches of the conduits

$$0.25f < f_{Ex} < 0.35\,f\ ;\ f = n/60$$

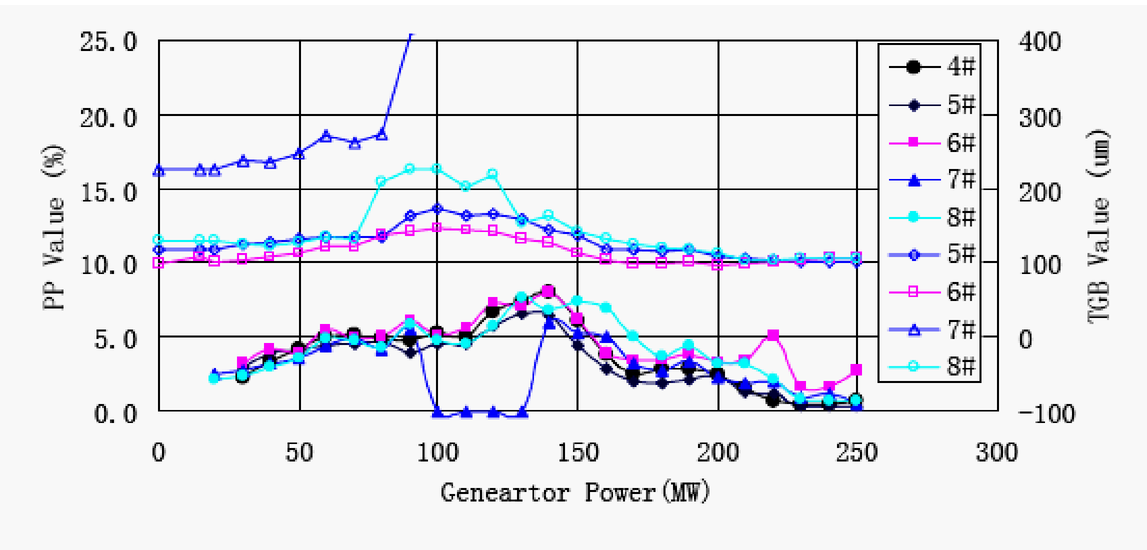

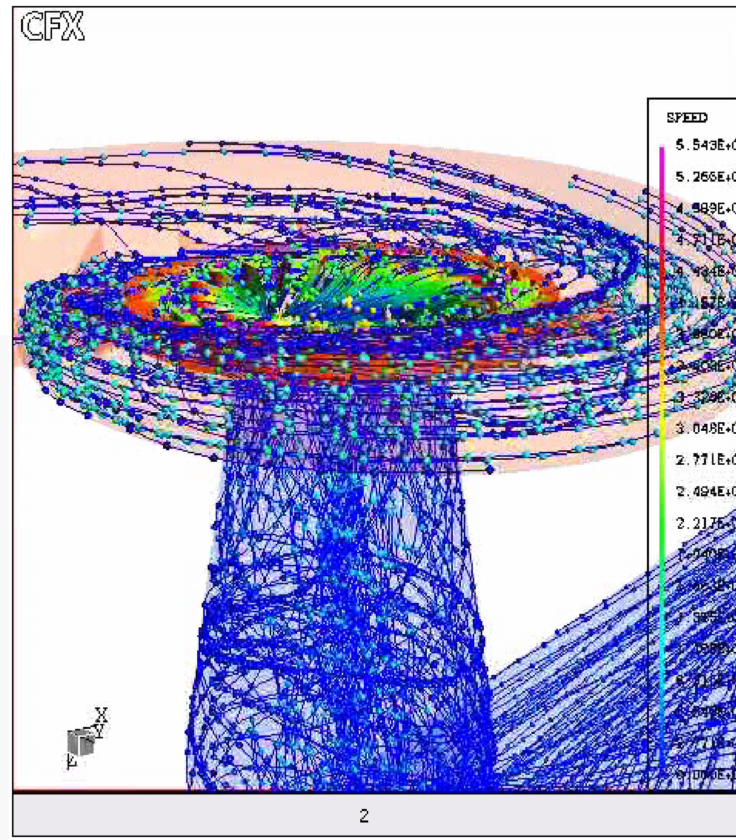

2.4 Pressure Pulsation (Cont'd)

- The measured pressure pulsation is equal 6.4 % (49 Kpa) and thus:

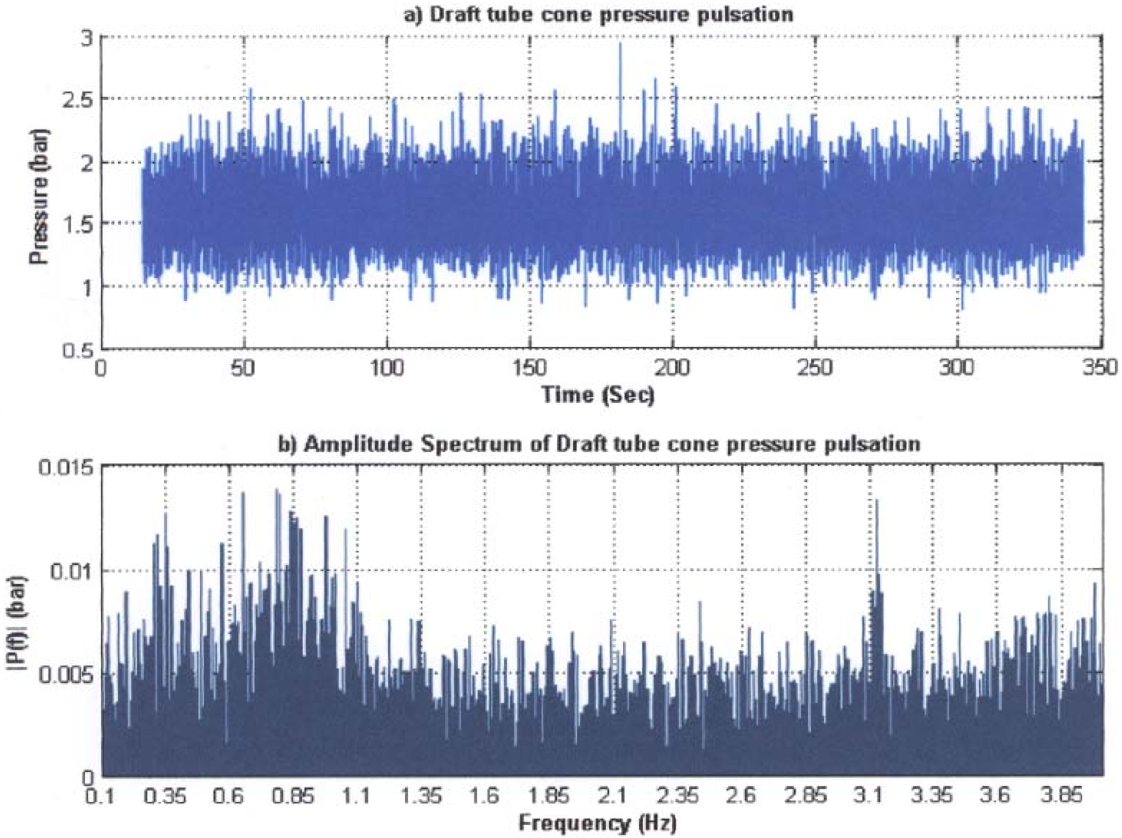

2.4 Pressure Pulsation (Cont'd)

- Associated with fluctuation of:
  - Shaft Torque
  - Rotational Speed
  - Load on Guide Vanes
  - Etc…

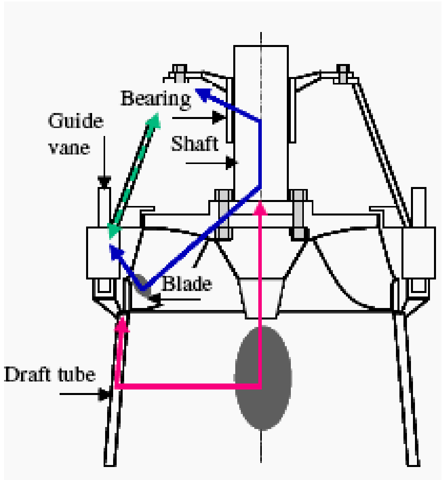

- Special Interest for Low Frequencies
  - Propagation in the water conduits& rotating parts
- Special Interest for Mechanical Vibrations
  - Structural Fatigue

2.4 Pressure Pulsation (Cont'd)

- **The pressure distribution in the draft tube :**
  - **Pressure pulsation of helical vortex Rotational Speed**
  - **Eccentricity of the rotation axis of helical vortex with respect to unit axis**

$$P(r,\theta) = P_{\min} + \Delta P'_{\max}\left(\frac{r-e}{R+e}\right)^2 + \left\{\Delta P'_{\max}\left(\frac{r+e}{R-e}\right)^2 - \Delta P'_{\max}\left(\frac{r-e}{R+e}\right)^2\right\}\left(\theta/\pi\right)^2$$

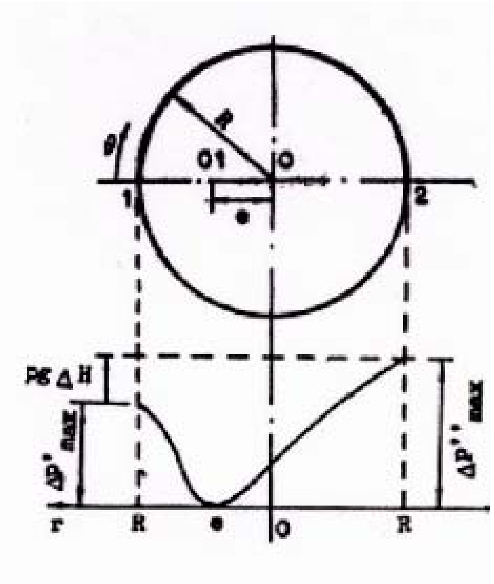

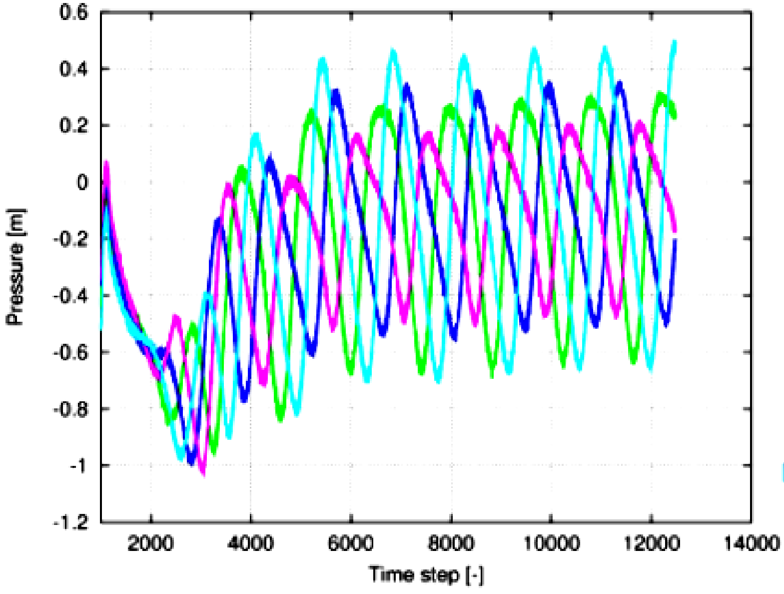

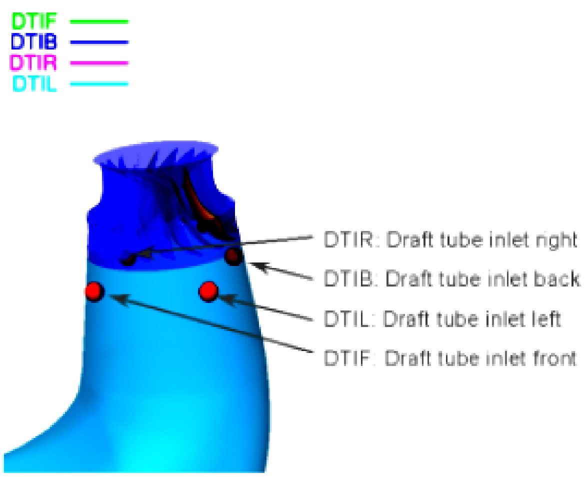

2.5 Resonance

- Oscillation modes in the reaches of the conduits

$$f = \frac{i.a}{4.L}$$

with i = 1 , 3 ,5 ,….

L: length of the conduit under consideration

a: wave propagation velocity.

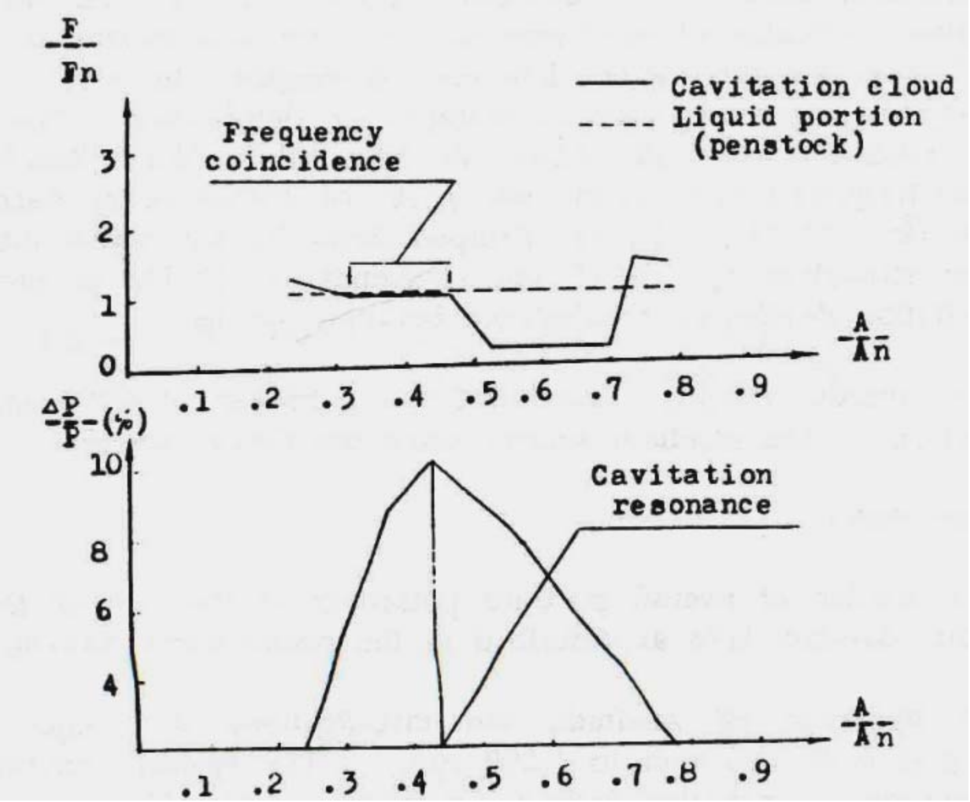

2.5 Resonance (cont’d)

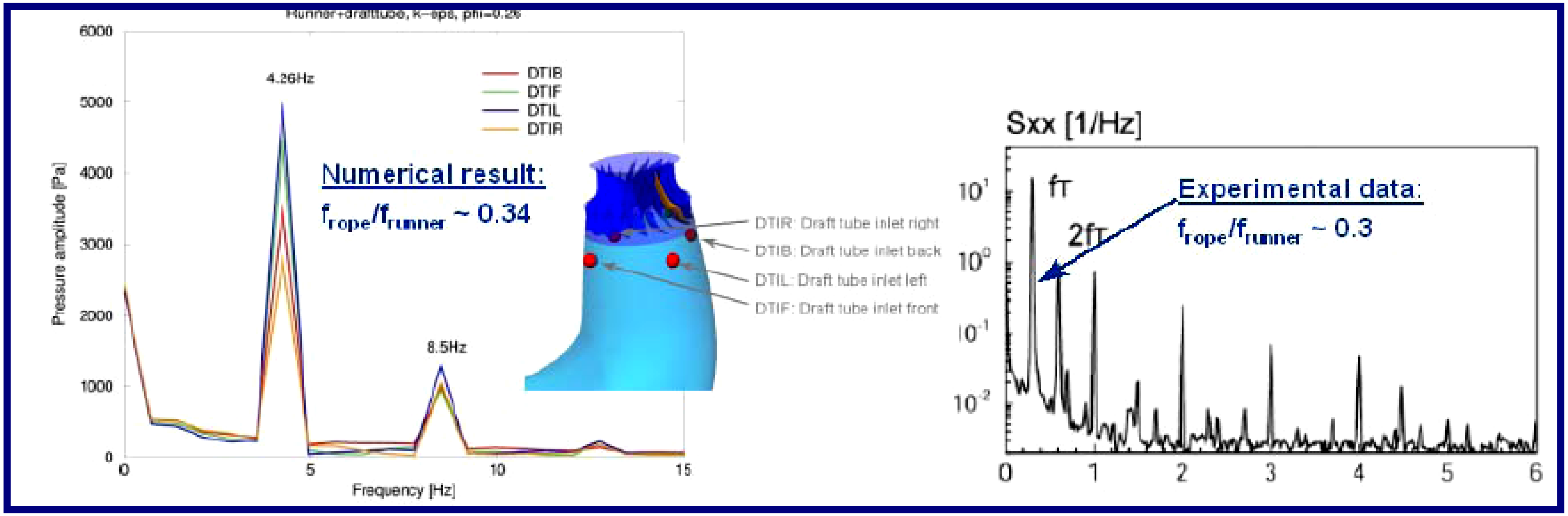

2.5 Resonance (cont'd)

- **Dynamic response analysis**
  - A mathematical model was set up to investigate the oscillatory behavior of the systems
  - The model is based on the impedance Method

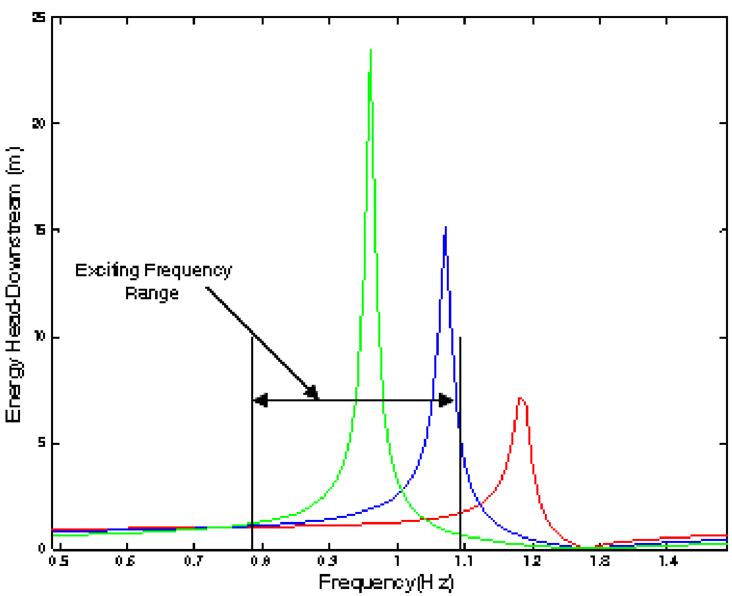

$$Zc = \frac{a}{g.A}.\sqrt{1 - j.\frac{\lambda.Q_0}{\varpi.D.A}}.$$

$$\alpha = \frac{j.\varpi}{a}.\sqrt{1 - j.\frac{\lambda.Q_0}{\varpi.D.A}} = \frac{j.\varpi.g.A}{a^2}$$

$$h(x) = \cosh(\alpha.x).ha - Zc.\sinh(\alpha.x).qa$$

$$q(x) = -\sinh\frac{(\alpha.x)}{Zc}.ha + \cosh(\alpha.x).qa$$

2.6 Effects of Pressure and Sound Speed (cont'd)

- Equal Intensity
- The sound speed in the medium

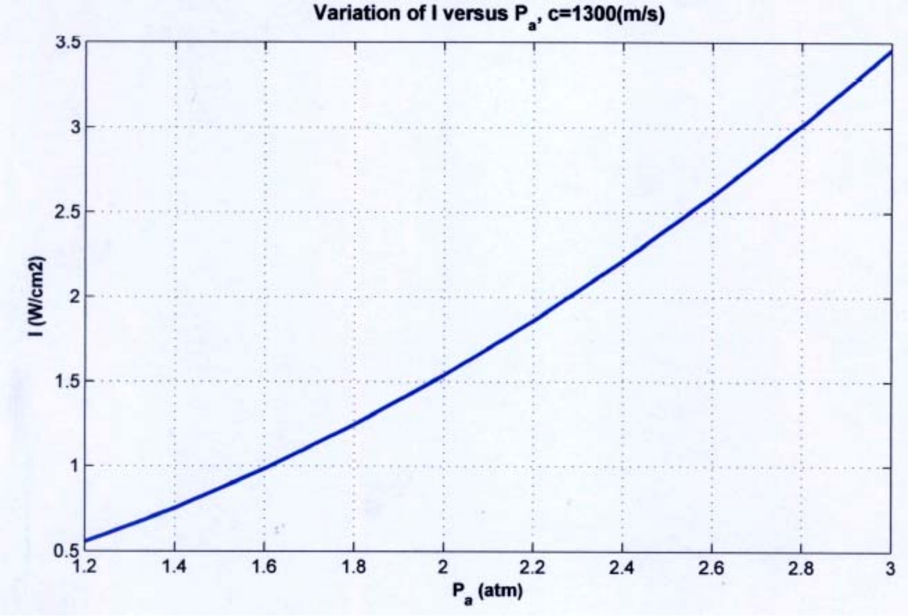

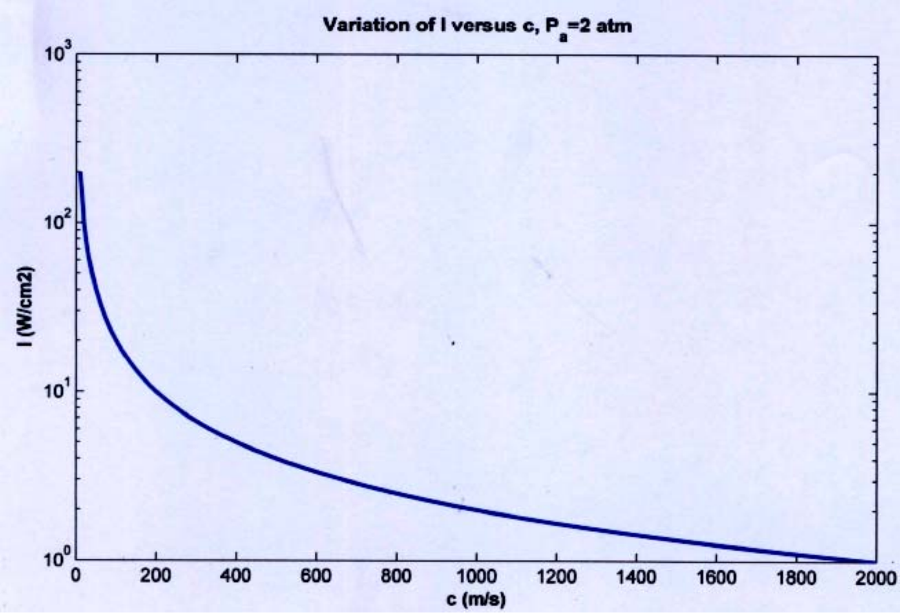

3 -Bubbles released within a Helical Vortex Field

- Effective parameters on the non linear nature of the bubble motion and capture by helical vortex:
  - **3.1 Bubble size**
  - **3.2 The role of the initial bubble position on its trajectory around the vortex**
  - **3.3 Bubble capture by helical vortex field**
  - **3.4 Non-spherical deformation and elongation by vortex effect**
  - **3.5 Comparison between bubble behavior in vortex flow field and generated by acoustic wave**

3.1 Bubble Size

- **It is simulated releasing a bubble away the vortex center in a Rankin line vortex axial Velocity**
  - bubble capture by the vortex
  - interaction between the vortex and a bubble
  - dynamics of elongate bubbles on the vortex axis

- **Tangential velocity vθ around the vortex axis and the corresponding pressure field**

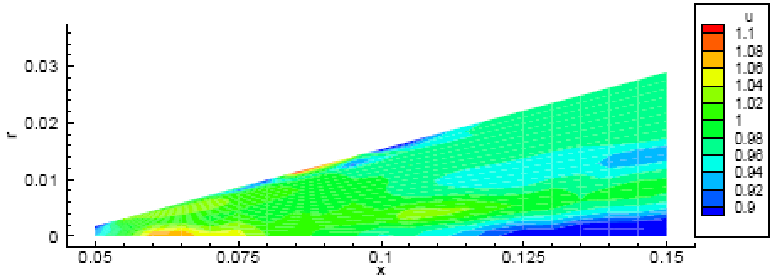

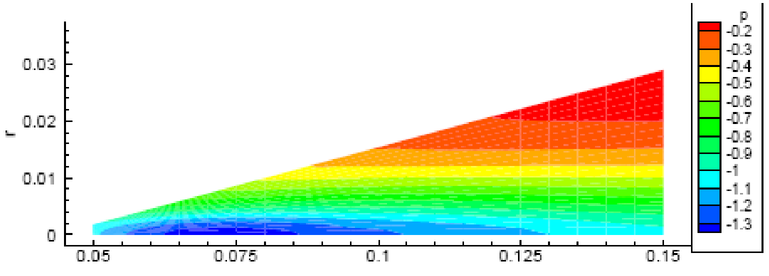

3.2 The role of the initial bubble position on its trajectory around the vortex

- **Bubble capture depend on**
  - Bubble size
  - Distance of vortex axis

- **Bubble Trajectory**
  - Quick Capture
  - Slow Capture

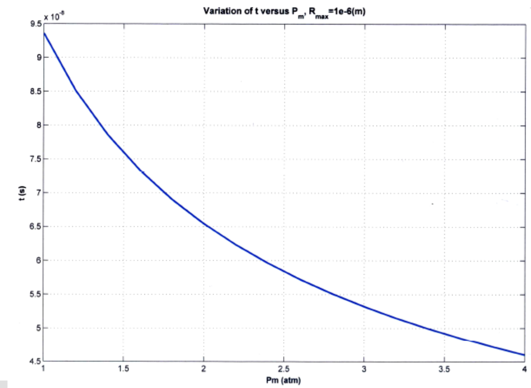

$$\tau = 0.915 R_0 \sqrt{\frac{\rho}{p_\infty - p_v}}$$

Rayleigh time or collapse time, τ
bubble reaches a maximum radius, R_0

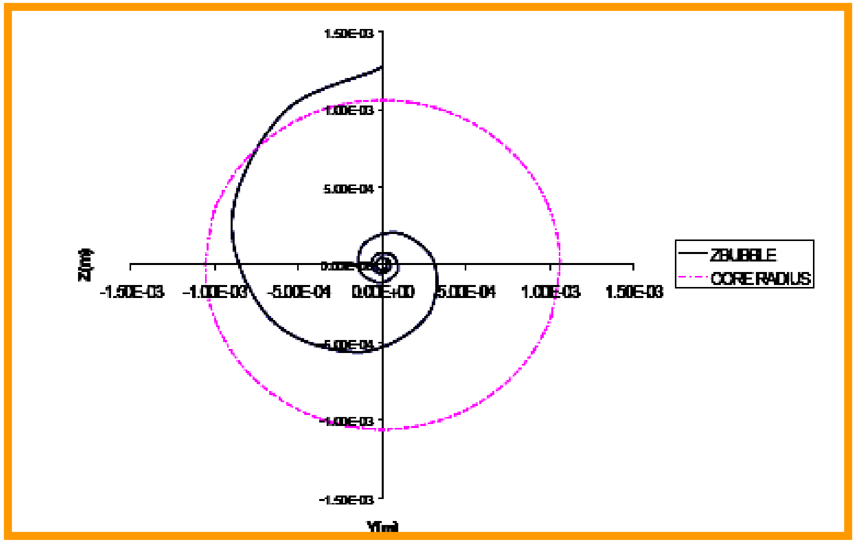

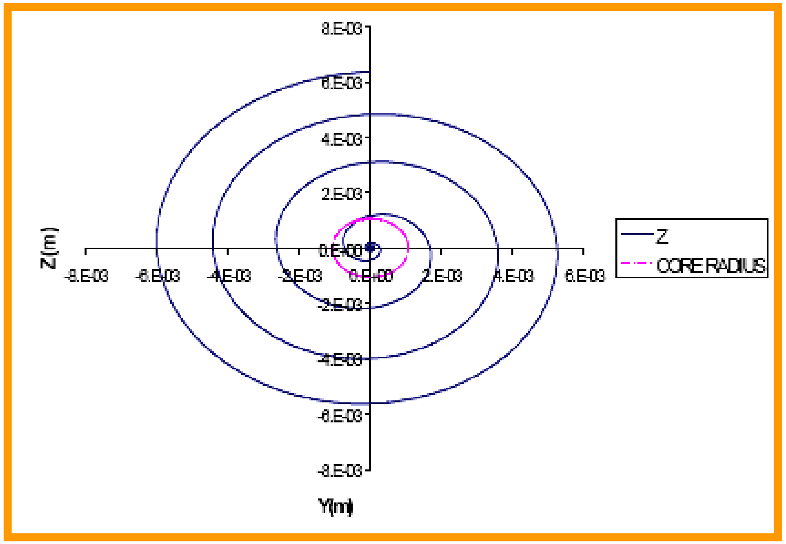

3.2 The role of the initial bubble position on its trajectory around the vortex (cont'd)

- Interaction between the vortex and a bubble
  - A surface Average Pressure (SAP) spherical bubble dynamics model based on the Rayliegh-Plesset equation was developed and successfully applied to study the bubble dynamics in a vortex flow

$$(1-\frac{\dot{R}}{c})R\ddot{R}+\frac{3}{2}(1-\frac{\dot{R}}{3c})\dot{R}=\frac{(\mathbf{u}-\mathbf{u}_b)^2}{4}+\frac{1}{\rho}(1+\frac{\dot{R}}{c}+\frac{R}{c}\frac{d}{dt})\left[p_v+p_{g0}\left(\frac{R_0}{R}\right)^{3k}-p_{encounter}-\frac{2\gamma}{R}-4\mu\frac{\dot{R}}{R}\right]$$

C : Sound speed

R_0 : Initial bubble radius

P_v : Vapor pressure

P_{g0}: Initial gas pressure inside the bubble

P_{en}: Ambient pressure “felt” by the bubble during its travel

K : Polytropic gas constant (k=1.4)

$(u-u_b)^2/4$:Additional pressure due to slip velocity between the liquid and bubble

3.2 The role of the initial bubble position on its trajectory around the vortex (cont'd)

- Interaction between the vortex and a bubble
  - 1 - Bubble Motion equation

$$\frac{d\mathbf{u_b}}{dt} = \frac{3}{\rho}\nabla P + \frac{3}{4}C_D\left(\mathbf{u}-\mathbf{u}_b\right)\ \left|\ \mathbf{u}-\mathbf{u}_b\right| + \frac{3}{R}\left(\mathbf{u}-\mathbf{u}_b\right)\dot{R}$$

Ub: Bubble traveling velocity

CD: Drag Coefficient

R : Time varying bubble radius

  - 1 – Rankine Vortex Model
  - Close to the vortex rotation center the vector field behaves like a solid body rotation.
  - Tangential velocity grows linearly with respect to r.
  - Beside a distance r=r_v (the vortex core radius), the tangential velocity decays

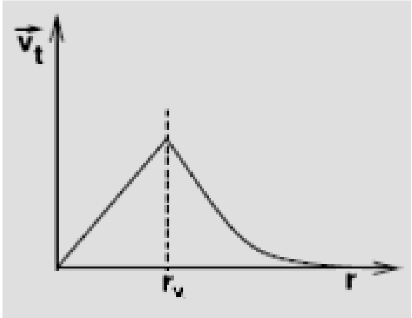

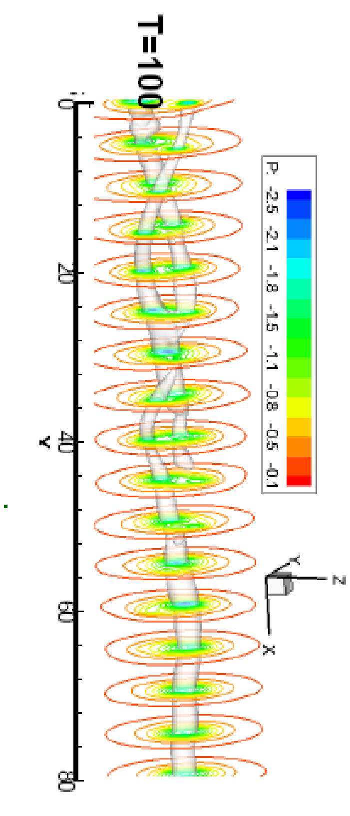

Pressure contours

3.3 Bubble Capture by Helical Vortex Field

Force Vortex Region

$$vu = \frac{r\Gamma}{2\pi r^2}$$

$$p = \frac{p\Gamma^2\left(r^2 - r_c^2\right)}{8\pi^2 r_v^4} + P_c$$

Free Vortex Region

$$Vu = \frac{\Gamma}{2\pi r}$$

$$p = \frac{p\Gamma^2}{8\pi^2}\left(\frac{1}{r_v^2} - \frac{1}{r^2}\right) + \frac{p\Gamma^2\left(r_v^2 - r_c^2\right)}{8\pi^2 r_v^4} + p_c$$

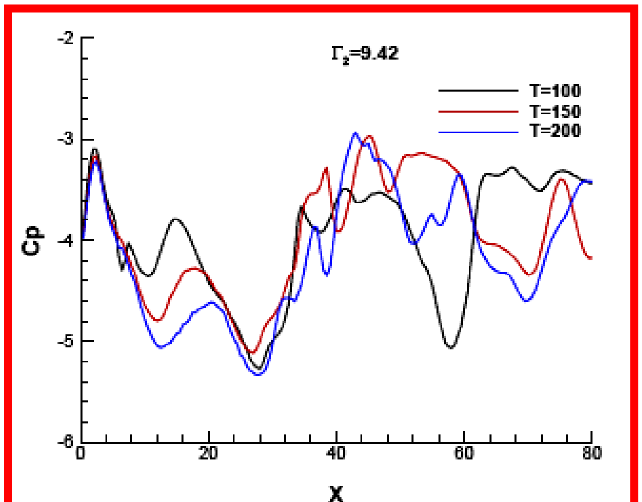

Local minimum pressure coefficients for Γ_2=9.42

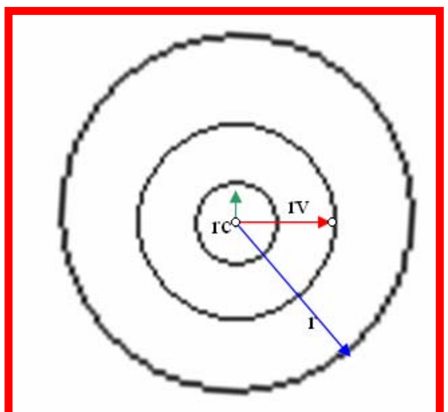

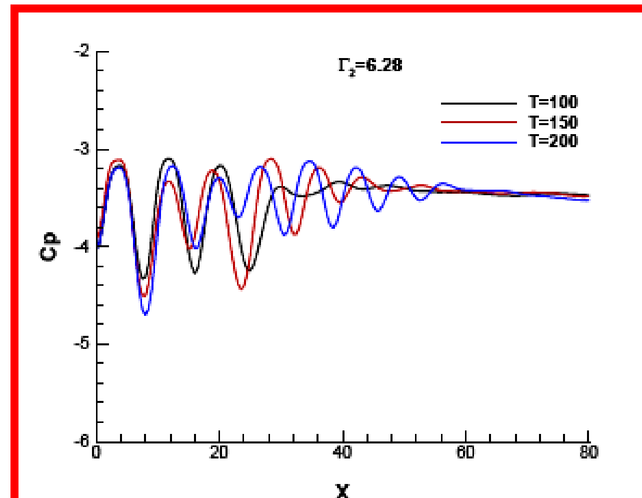

Local minimum pressure coefficients for Γ_2=6.28

3.3 Bubble Capture by Helical Vortex Field (cont'd)

▪Shape Factor

❖Suppose a bubble slightly deformed from its original spherical shape due to pressure field of the vortex
❖The shape factor can be easily calculated while the bubble

$$R_{local} = \frac{2\gamma}{p_v + p_g - p_{local}}.$$

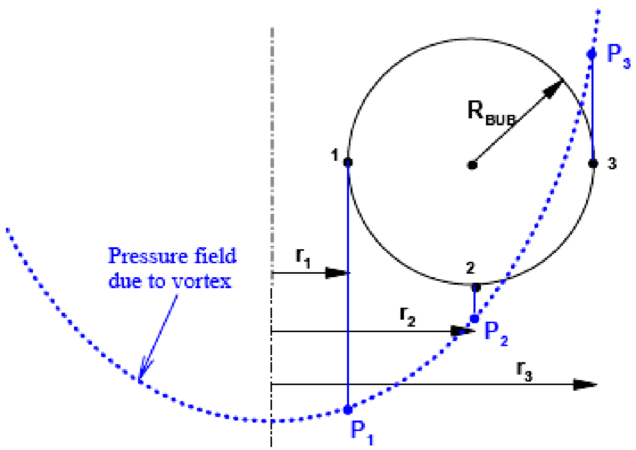

$$p_v + p_g = p_{local} + 2\gamma / R_{local}$$

$$SF \equiv \frac{R_{local}}{R_{bub}}.$$

3.4 Non-Spherical Deformation and Elongation by Vortex Effects (cont'd)

- **A bubble placed on the vortex axis usually elongates along this axis**
- **Often elongation is so extreme that the bubble eventually splits into smaller sub-bubbles.**
- **The mid part of bubble becomes concave, and the bubble eventually splits two sub-bubble.**
- **Both of the sub-bubbles develop axial jets from the split, one propagate upstream and the down stream.**
- **The jets later touch the other side of the sub-bubble on the axis.**

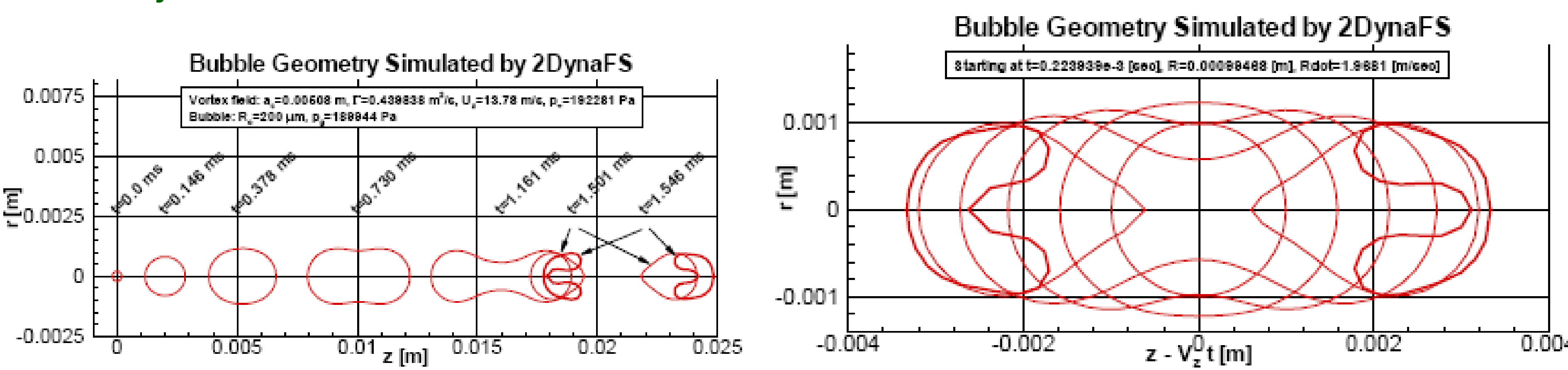

(a) (b)

Figure : The bubble behavior in a vortex flow field; (a) a spherical bubble of 200 *μm* released at the origin, and (b) a bubble started 0.224 *ms* later with initial radius 947 *μm* and initial radial velocity 1.968 *m/s*.

3.3 Bubble Capture by Helical Vortex Field (cont'd)

- The bubbles released at off axis location is captured by the vortex, arriving at the axis at about 1ms after release.
- As the bubbles moves along the vortex axis, it experiences a sudden growth after t=2 ms, followed by multiple collapse and rebounds with the emission of strong pressure pulses.

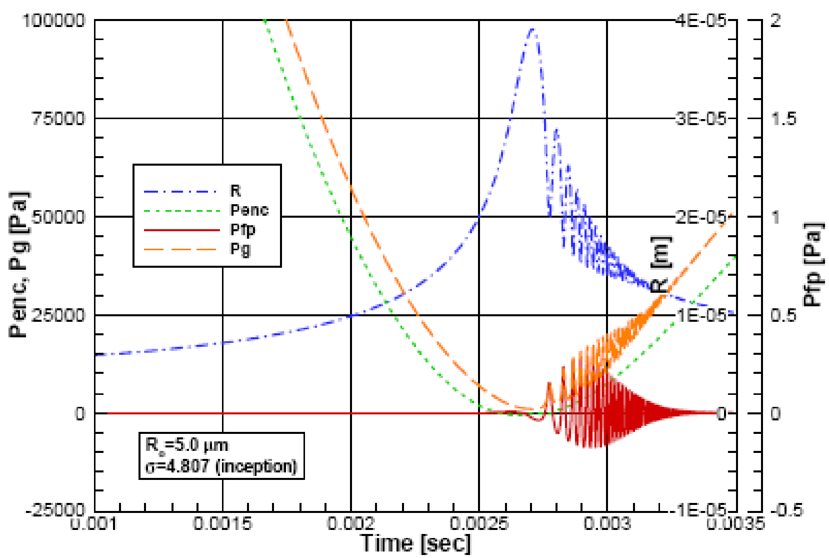

Figure : Bubble behavior predicted by the SAP spherical model. (R: bubble radius, Penc: encounter pressure, Pfp: field point pressure at (*z*,*r*)=(0,0.3) *m*, Pg: gas pressure inside the bubble)

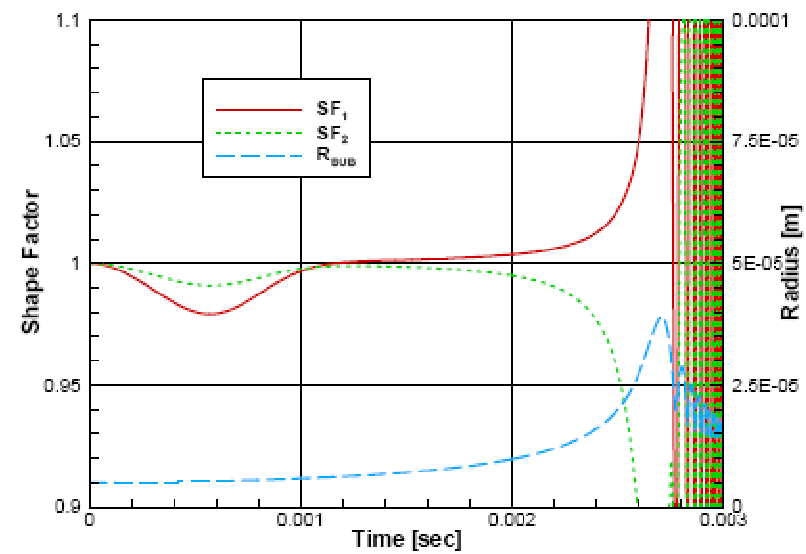

Figure : Shape factors calculated by the SAP spherical model. (R_{BUB}: spherical bubble radius, $SF_{1,2}$: shape factors defined by equation (6) for points 1 and 2 shown in Figure 2.)

3.4 Non-Spherical Deformation and Elongation by Vortex Effects

- Bubble splitting behavior ,bubble size before and after splitting ,and emitted pressure signals are characterized in a wide range of cavitation numbers
- The effect of the Reynolds number the effect of initial bubble nucleus size are also investigated.
- These reentrant jets result in pressure pulse emissions which are orders of magnitude higher than those due to spherical bubble dynamics.

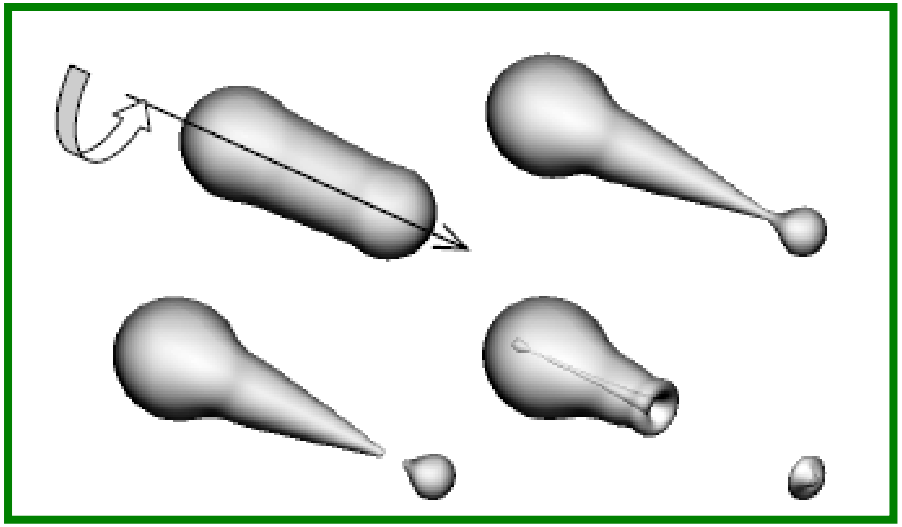

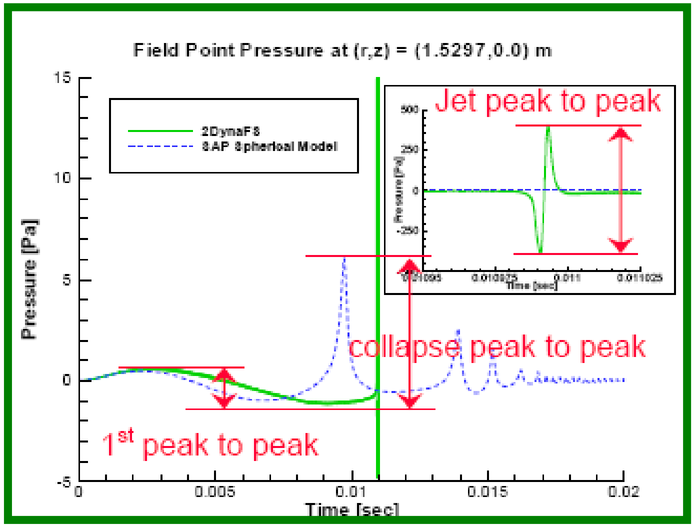

3.4 Non-Spherical Deformation and Elongation by Vortex Effects

- The bubble size versus time is shown by using a volume equivalent bubble radius for the non-spherical bubbles.
- For the cavitaion number 2.50, the bubble experiences splitting shortly after reaching its maximum size, while a single reentrant jet forms for cavitation number 2.54 at the downstream end of the bubble.
- When the cavitation number is very close to inception no splitting occurs.

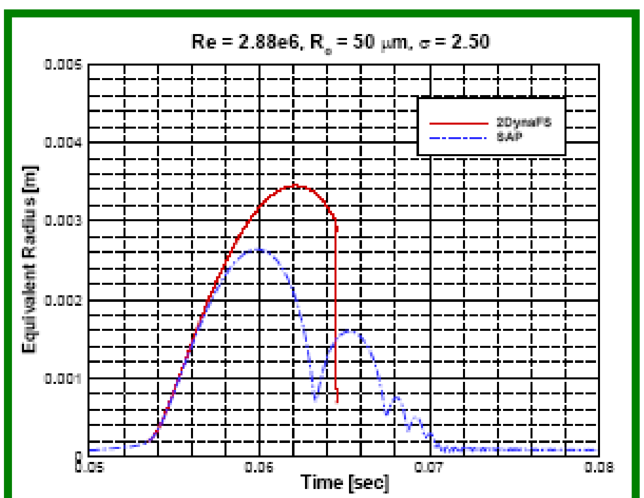

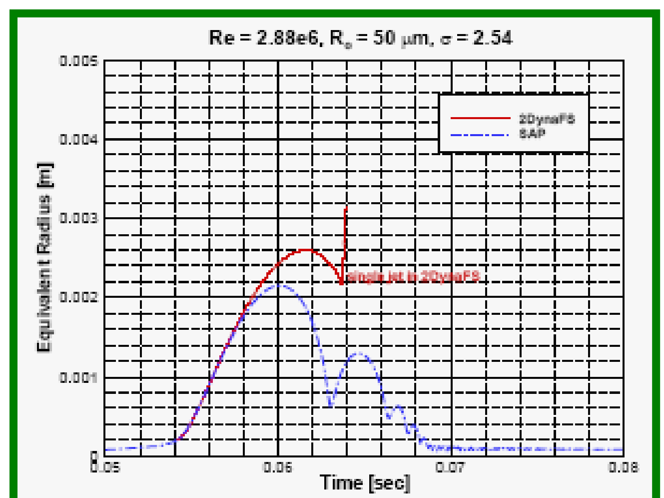

3.4 Non-Spherical Deformation and Elongation by Vortex Effects (cont'd)

- The peak-to-peak values of the pressure at the field pint for a range of cavitation numbers are compared.
- Overall the flattening trend towardthe lower cavitation numbers is observed for ll pressure peaks.

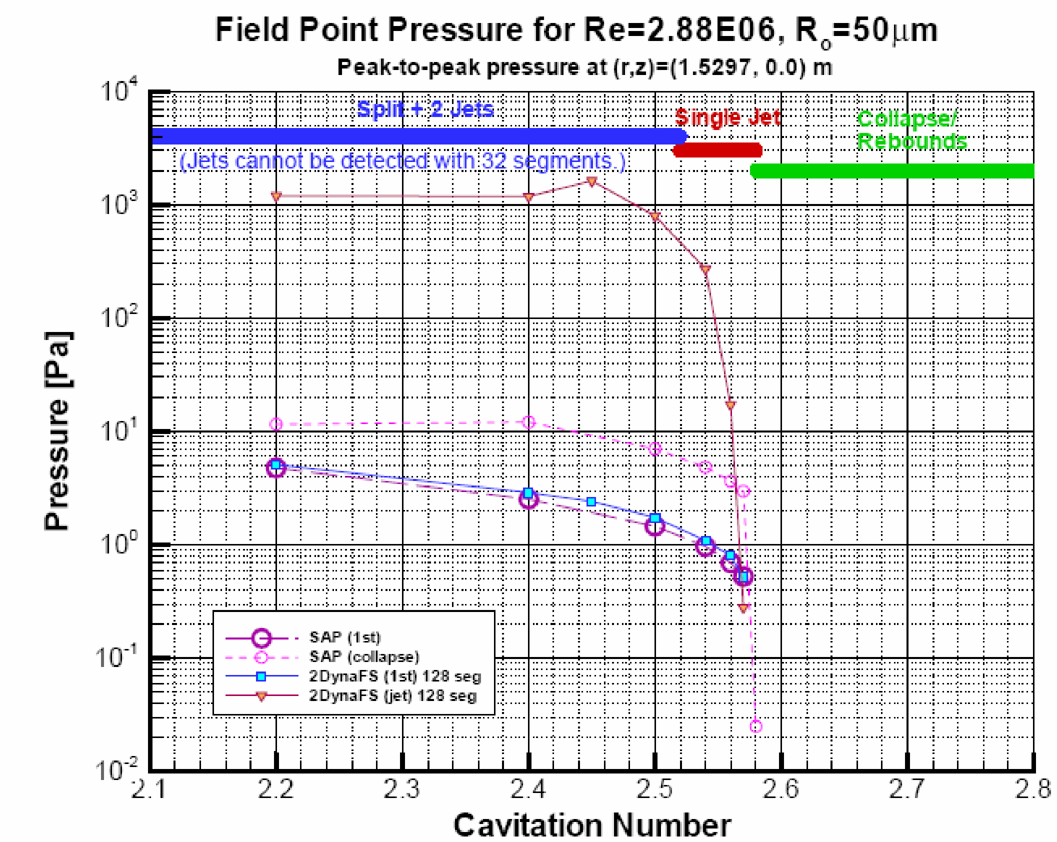

3.4 Non-Spherical Deformation and Elongation by Vortex Effects (cont'd)

- The maximum radius of the bubble reached a given σ,as well as its radius of the sub-bubbles generated

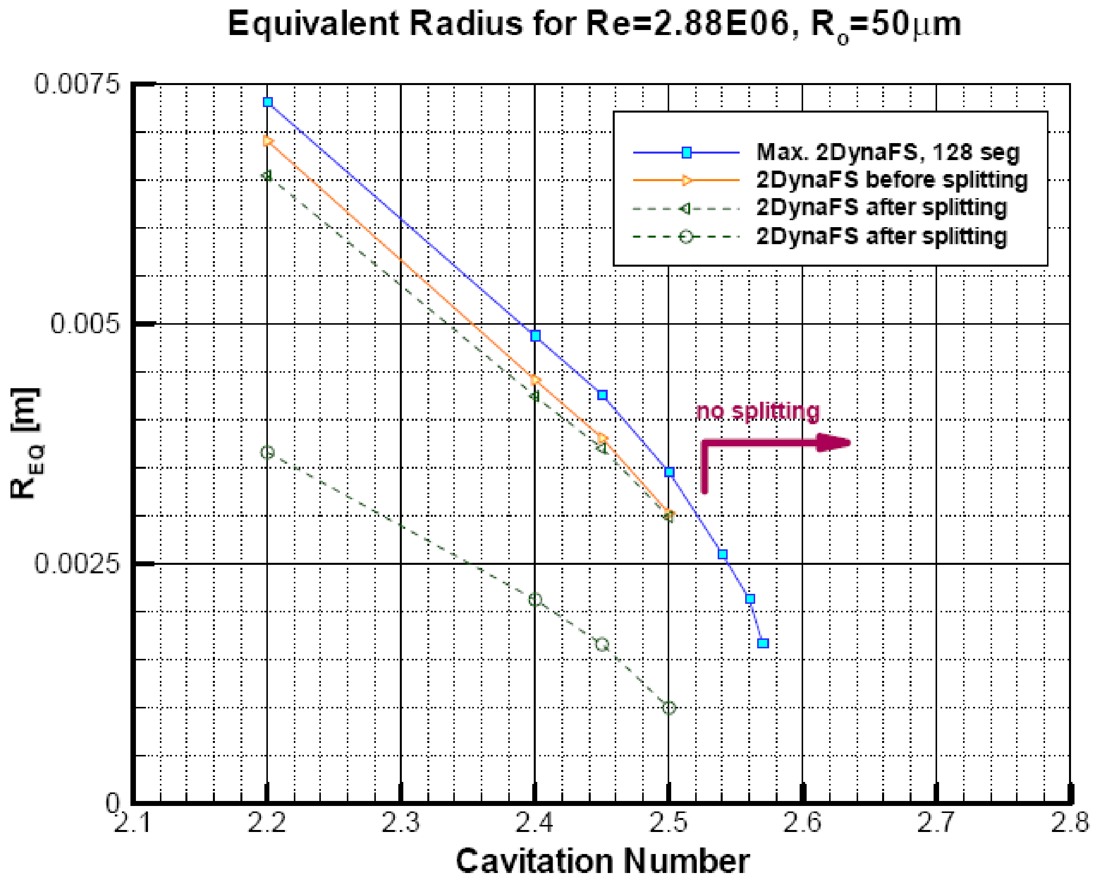

3.4 Non-Spherical Deformation and Elongation by Vortex Effects (cont'd)

- Comparison of the equivalent radius for four initial bubble sizes, 10,20,50 and 100 μm and to foreseen the equivalent radius for load rejection case in the hydro turbine.

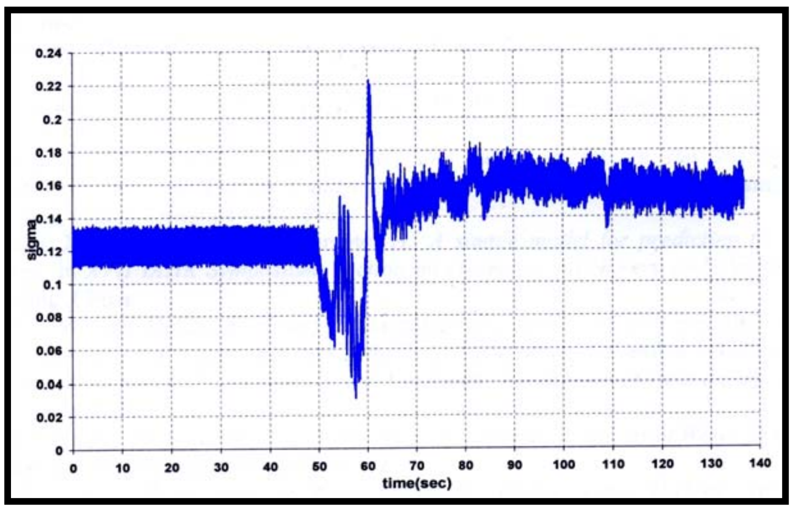

Cavitation number in draft tube of turbine during load rejection

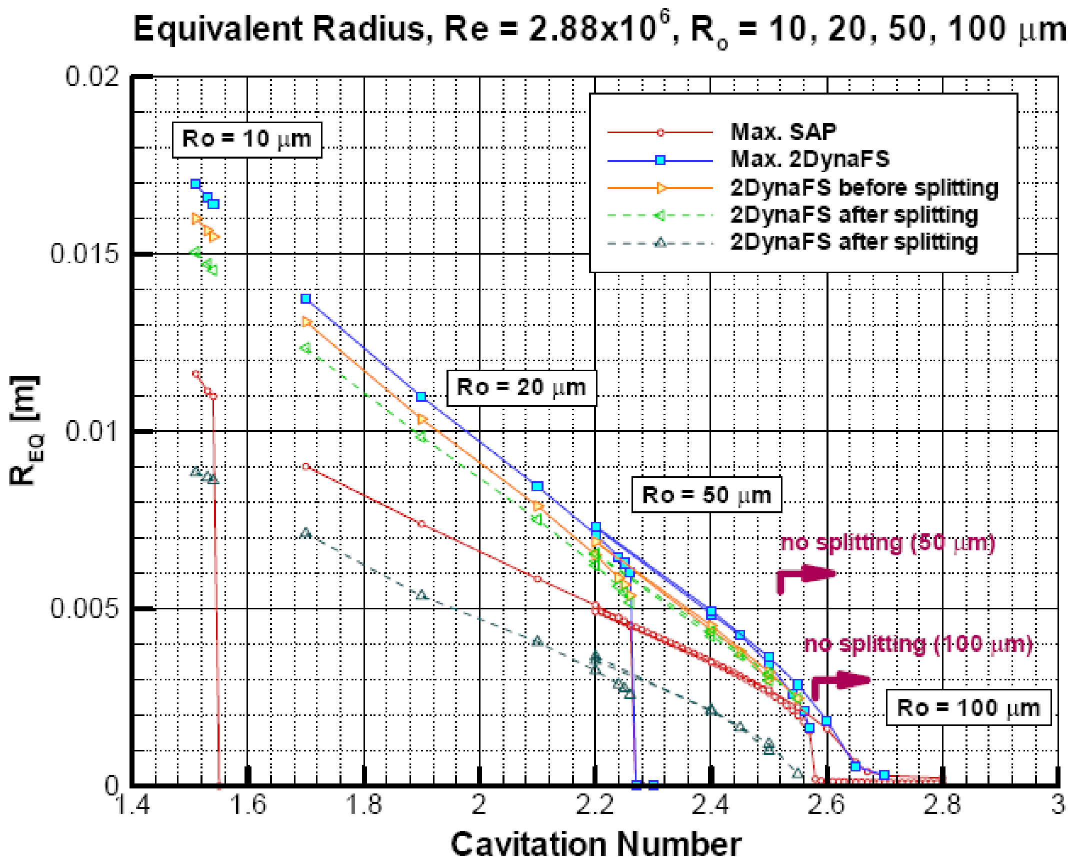

3.4 Non-Spherical Deformation and Elongation by Vortex Effects (cont'd)

- The cavitation coefficient effects on helical vortex
- The probability of bubble capture by vortex increase as the cavitation numbers decrease during load rejection associated with resonance

$\sigma = 0.38$ $\sigma = 0.70$ $\sigma = 1.18$

Waterfall diagram and corresponding cavitation ropes

3.4 Non-Spherical Deformation and Elongation by Vortex Effects (cont'd)

- The bubble behavior shown on the left figure is viewed from an observer moving with the constant axial velocity of the vortex field.
- The pressure signal , shown on the figure , also presents the oscillation of the bubble in the period of 0.92 micro second. This phenomenon seems to generate the bubbles with radius less than 1 μm.
- The amplitude of the oscillation increases as the bubble moves downstream because ambient pressure becomes lower at downstream locations.

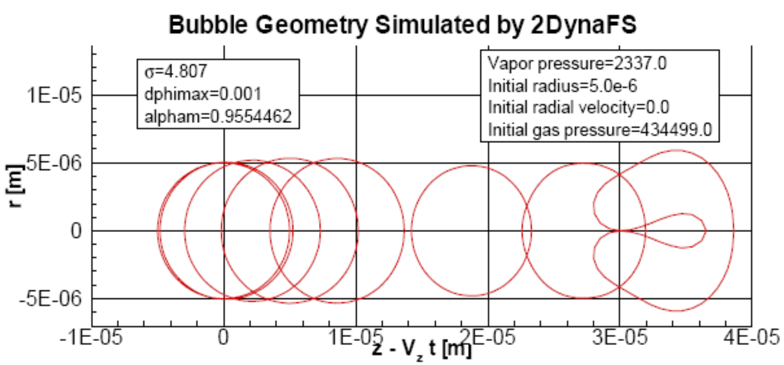

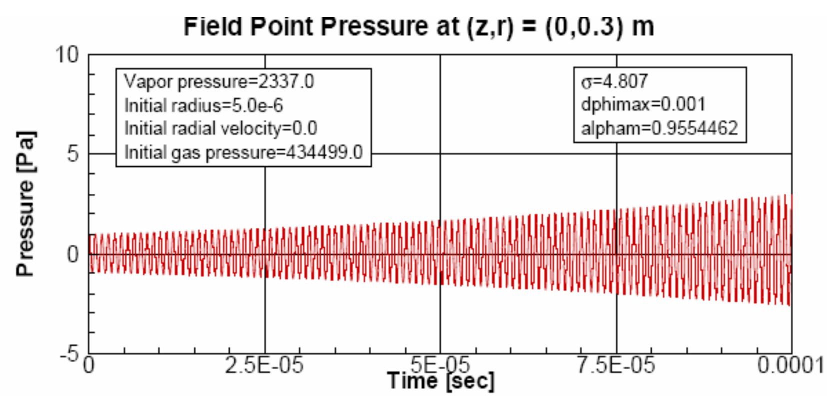

3.4 Non-Spherical Deformation and Elongation by Vortex Effects (cont'd)

- It is simulated releasing a bubble away the vortex center in a Rankin line vortex axial Velocity

Figure: Bubble shape and location during its capture by a line vortex, as obtained for bubble initially off the vortex center, Ro=200 μm,P_{g0}/P_{∞}=1 and σ=2.0

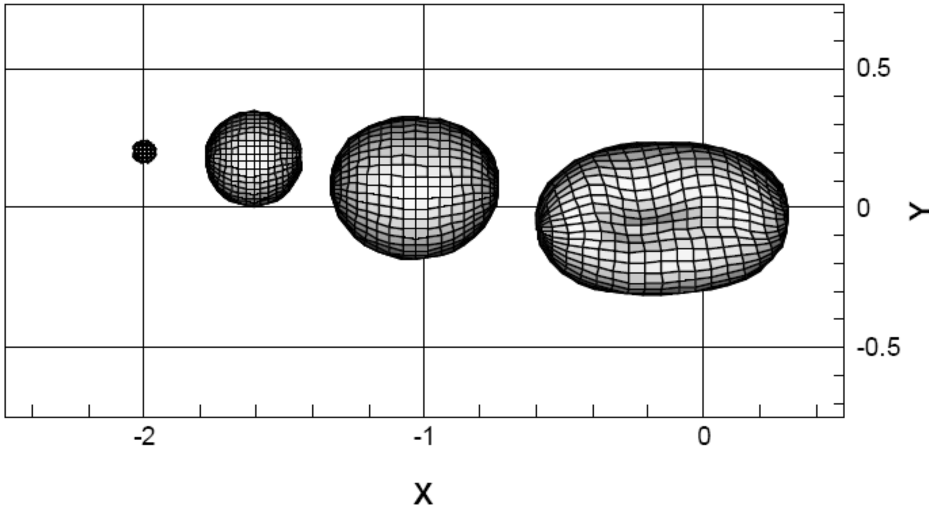

Figure: Pressure and Velocity Contour

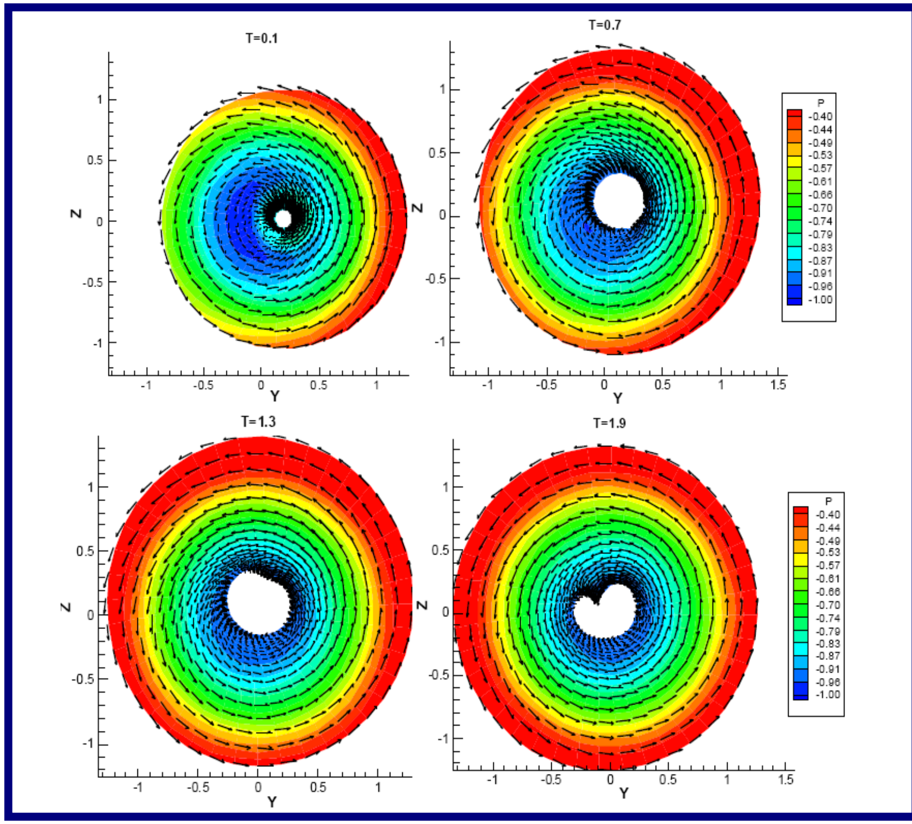

3.4 Non-Spherical Deformation and Elongation by Vortex Effects (cont'd)

■ Jet Behavior

- It is clear from the figure that the N shape pressure signal after the split is closely related to the formation of the two axial jets shooting the opposite directions since the total volume of the bubbles remains more or less constant through this quick process,
- the source of the pressure signal is not the fluctuating volume but mainly the movement of the fluid mass due to the jets or the change in the volume liquid "sucked" into the sub-bubbles.

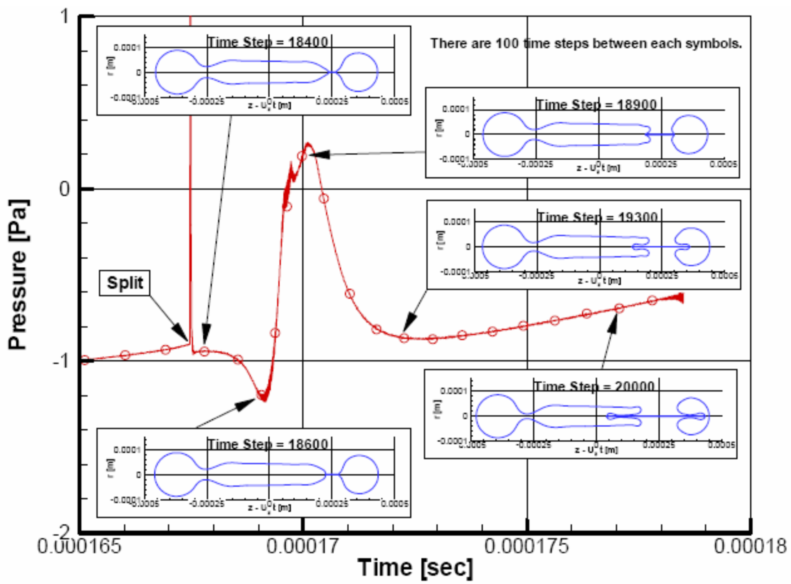

3.5 Comparison Between Bubble Behavior in Vortex Flow Field and Generated by Acoustic Wave

- **Shape history for bubble on force vortex region , Ro=200 μm,P_{g0}/P_{∞}=1 and σ=2.0**

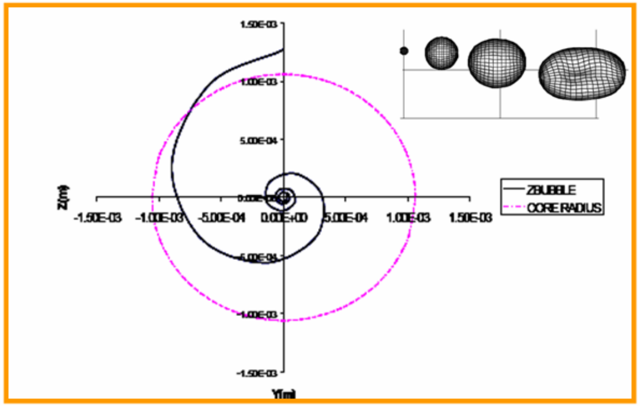

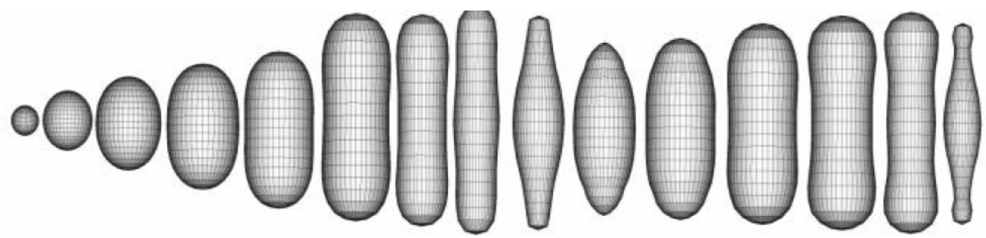

- **Bubble generated by acoustic wave**

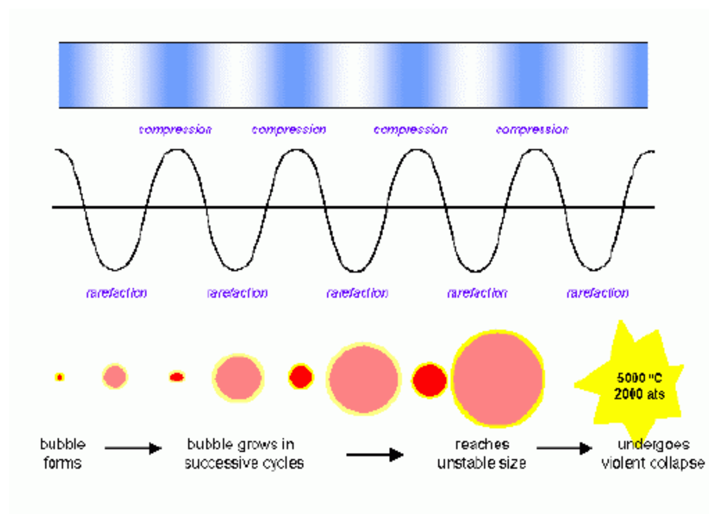

4 Cold Fusion Process in Hydro Machinery

- 4.1 Luminescence
- 4.2 water quality of river and chemical composition of runner
- 4.3 Cavitation Pitting
- 4.4 Jet Plasma
- 4.5 Cold Fusion Effects
- 4.6 PAZ (Plasma Affected Zone)
- 4.7 The Effects of Sigma and Reynolds

4.1 Luminescence

- The motion of a luminescing bubble involves the growth of a nucleus to a maximum size during low pressure
- Most of luminescence is emitted at the first collapse time by the main cavity.
- Emission occurs as short light bursts with a duration down to 10 ns and up to 100 ns luminescence emission ,
- in terms of detection success and intensity , is clearly increased with dissolved gas in water
- The vortex intensity is a driving parameter of the luminescence emission.

Type of SL	Medium	Spectrum character	Optical pulse width of SL flash	Number of photons per flash	Power per flash	Bubble temperature (K)	Acoust. ampl. (drive level)	Exp. ratio R_{max}/R_0	Inferred type of bubble motion
MBSL	Argon-saturated NaCl–ethylene glycol solution	Broadened asymmetric sodium D line emission	50 ns	10^6	7 μw	3×10^3 Comp. est.[24]	1 bar (low)	2.2 Est.[24]	*Soft collapse*
MBSL	Air-saturated ethylene glycol	Broadband extending from 350 to ~ 700 nm with a peak at 450 nm	1 ns	5×10^5	1 mw	5×10^3 Est. from Cr spectra[30]	3 bar (high)	5 Probable	*Hard collapse*
SBSL	Degassed water	Broadband extending from 200 to > 700 nm; No peak	100 ps	5×10^5	8 mw	2.5×10^4 Est. from blackbody fit to a spectrum[27]	1.4 bar (medium)	10 From experiments[9]	*Super collapse*
SBL (single bubble luminescence)	Degassed low vapour-pressure liquid	Broadband	< 1 ns	?	?	$> 10^6$ Desired	15 bar (high)	100 (see text)	*Hyper collapse*

4.1 Luminescence (cont'd)

- The investigation on blade of the luminescence was carried out by EPFL –IMHEF -Hydraulic Machine laboratory, Lausanne, in 2001

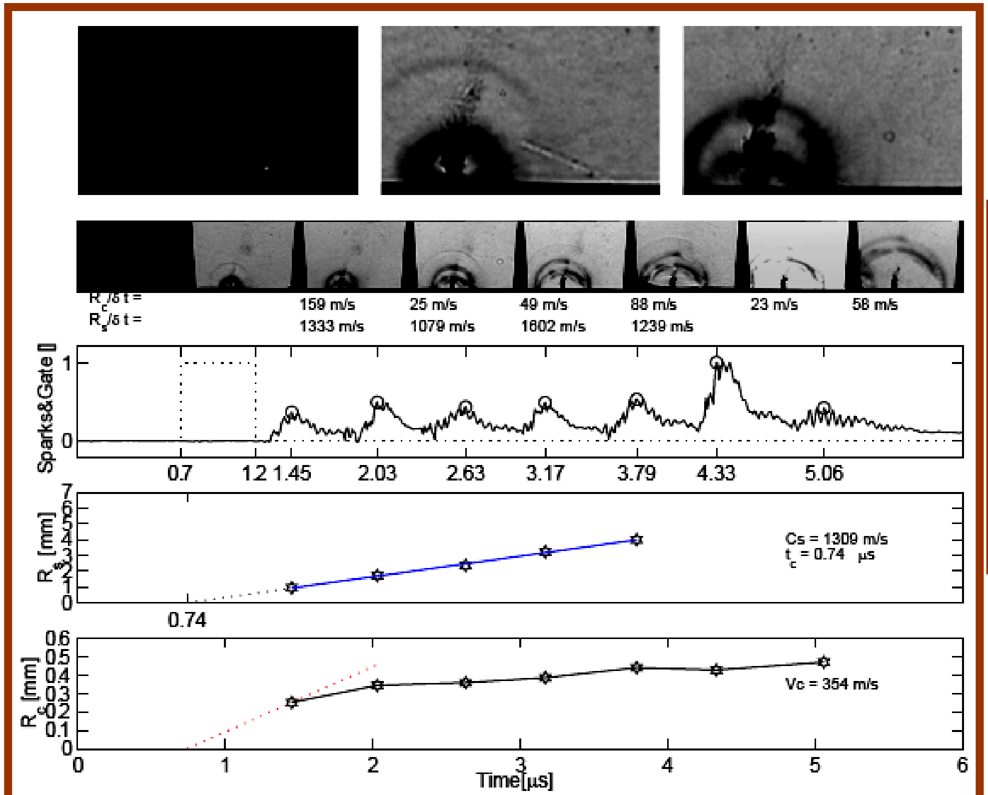

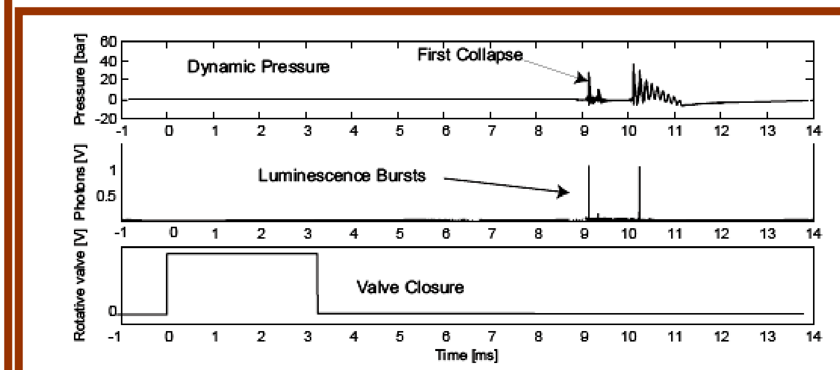

Simultaneous captures of luminescence and shock wave N=200 rpm, Q=0.66 l/s,

4.2 water quality of river and chemical composition of runner

Total dissolved solids	(mg/L)	376
Electrical conductance	$\mu S/cm@25^{o}C$	579
PH		7.81
Chloride	(mg/L)	2.29
Sodium	(mg/L)	2.33
Magnesium	(mg/L)	2.33
Calcium	(mg/L)	2.36
Sulfate	(mg/L)	0.8
Bicarbonate	(mg/L)	2.91

Water quality of river

Ni	Cr
10	18

The chromium and nickel percentage of weld metal

C	Mn	P	S	Si	Ni	Cr	Mo
0.06	1	0.035	0.0025	1	5	13.5	0.7

Chemical composition of runner GXCrNi13-4

4.3 Cavitation Pitting

- Cavitation bubbles implosion and fragmentation produce microregions of extreme conditions
- It is of importance for the bubble contents in this transient environment
- The parameters that are fundamental to this process are temperature, external pressure and collapse intensity
- The apparent increase of Luminescence is due to the increase of effective bubble production with respect to fusion.

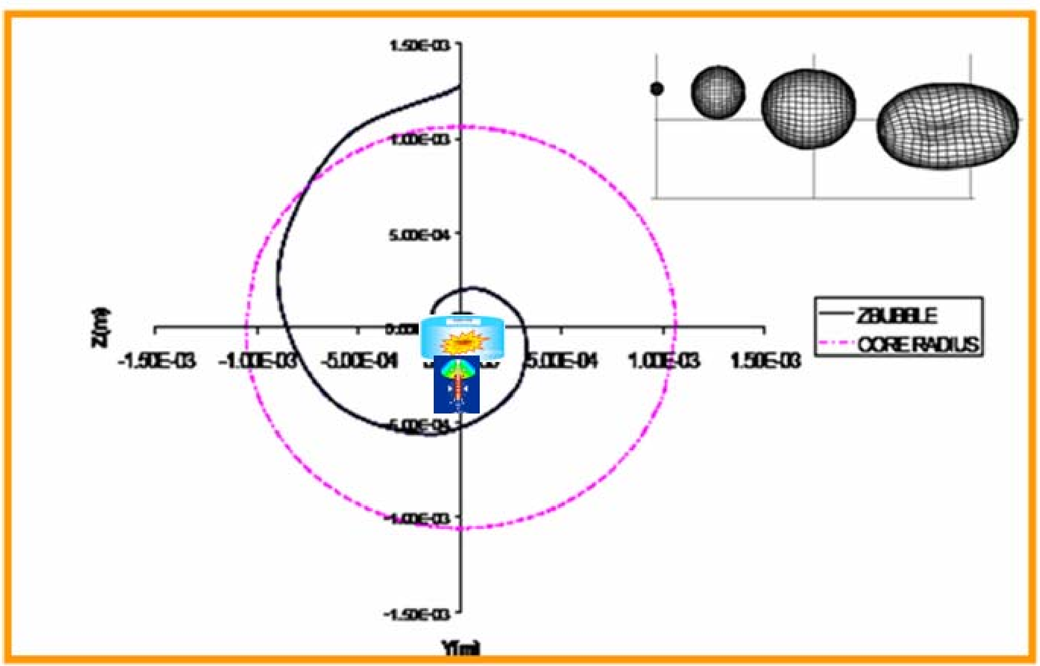

4.2 Cavitation Pitting

- The damages are generally termed cavitation or impingement erosion
- This process occurred in partial load operation and during load rejection with high pressure pulsation
- The jet accelerates (launched from the bubble collapse) toward the target foil as a plasma
- In this case ,the excess heat is released

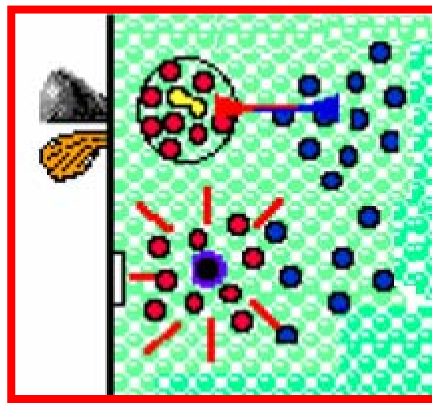

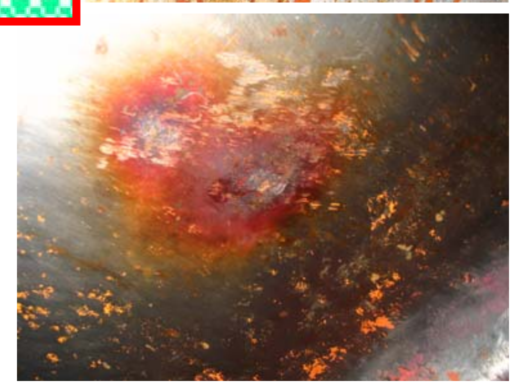

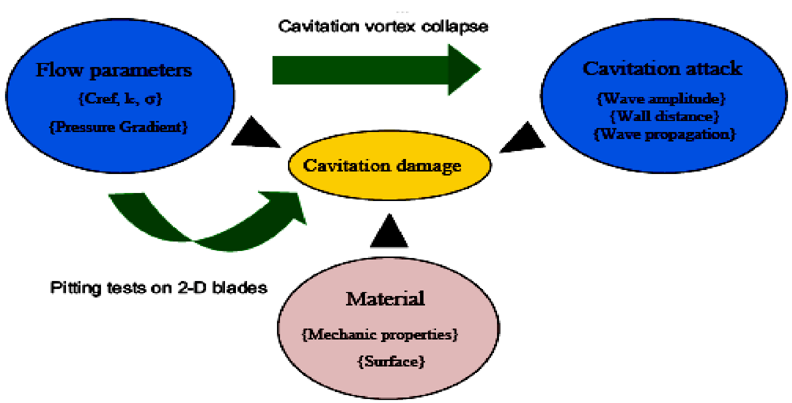

4.4 Jet Plasma

- **In the formation of hydrogen**
- **The hypothesis concerning the participation of :**
  - Alkaline metals and remaining substances in water river
  - It disintegrates water molecule into hydrogen and oxygen

$$H_2O \xrightarrow{)))} H + OH$$

  - Atomic nuclei of the runner blade material
  - Luminescence
  - The intensity of shock wave is more than the dynamic yield strength of the material

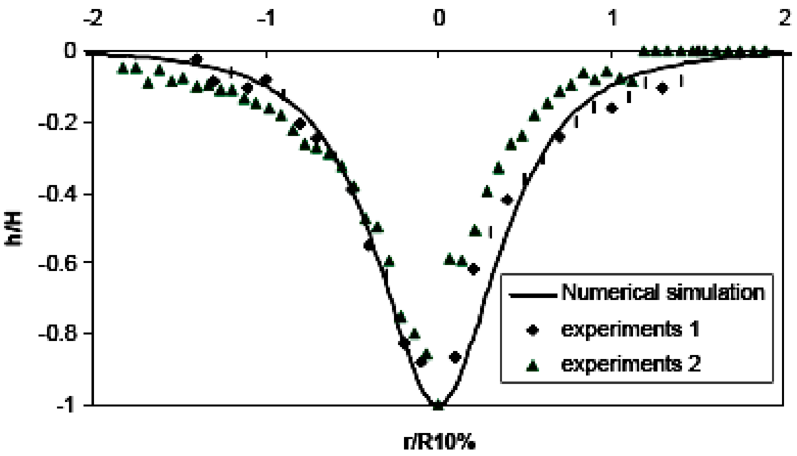

Permanent surface deformation calculated for pressure wave impact on material surface (H: pit depth ,R10%: Pit radius at 10% of H)

4.4 Jet Plasma (Cont'd)

- Atoms are destroyed by cavitation process or erosion
  - In partial load operation and during load rejection with high pressure pulsation
  - The protons of the destroyed nuclei begin to form the hydrogen atoms (on the basis of Dr. Mizunu and Dr. Kanarev hypothesis).
  - The appearance of the neutrons will promote the formation of the nuclei of deuterium, and, possibly, of tritium

- **During the transmutation of the iron nuclei, the atomic nuclei of chromium are formed**
  - When the atomic nucleus of iron pass into the atomic nucleus of chromium, two protons and two neutrons are released; two atoms of deuterium or one atom of helium can be formed from them
  - If the neutrons pass into the protons, four atoms of hydrogen are formed
  - the atomic nucleus of iron should lose two upper protons and two neutrons in order to pass into that atomic nucleus of chromium.

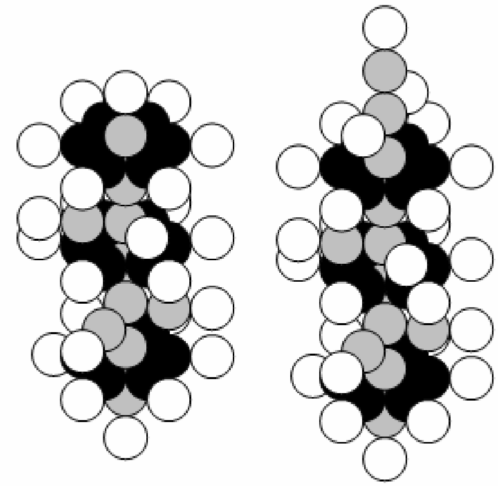

a) Cr (24,28) b) Fe (26,28)

4.4 Jet Plasma (Cont'd)

- The gases contact with plasma
  - Generation of a number of hydrogen micro-explosion almost at the same time
  - The quantity of burnt hydrogen determine the volume of generating hydrogen
  - Generation and explosion of hydrogen at pressure pulsation frequency
  - The impact force caused by hydrogen explosion and noise.

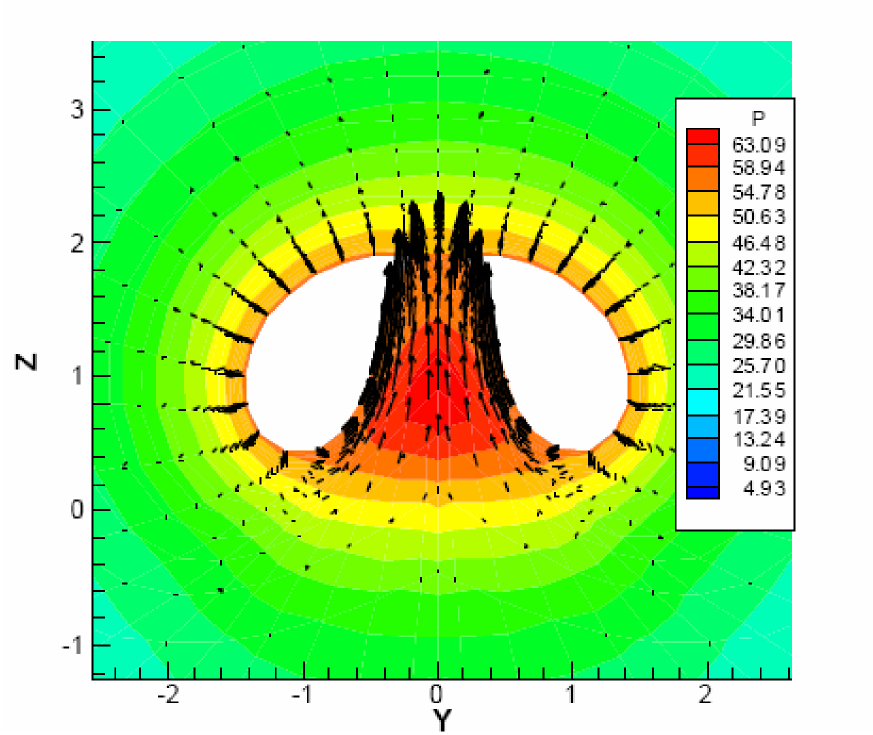

4.5 Cold Fusion Effects

- **A - Partial Load-Hydrogen Jet Plasma**
  - Impact on the runner and draft tube
  - Effects such as some cracks or pitting appear on the runner turbine and draft tube
  - Pressure pulsation frequency
  - Hydrogen generation

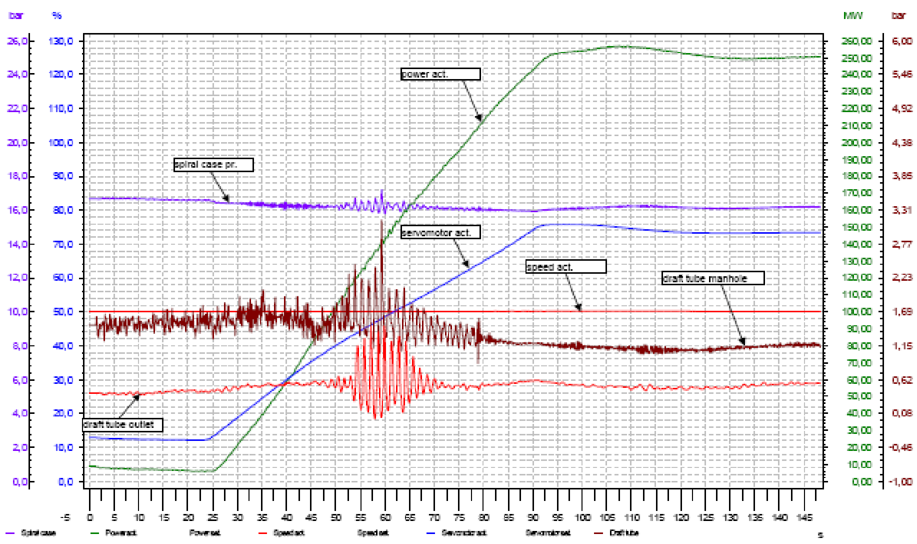

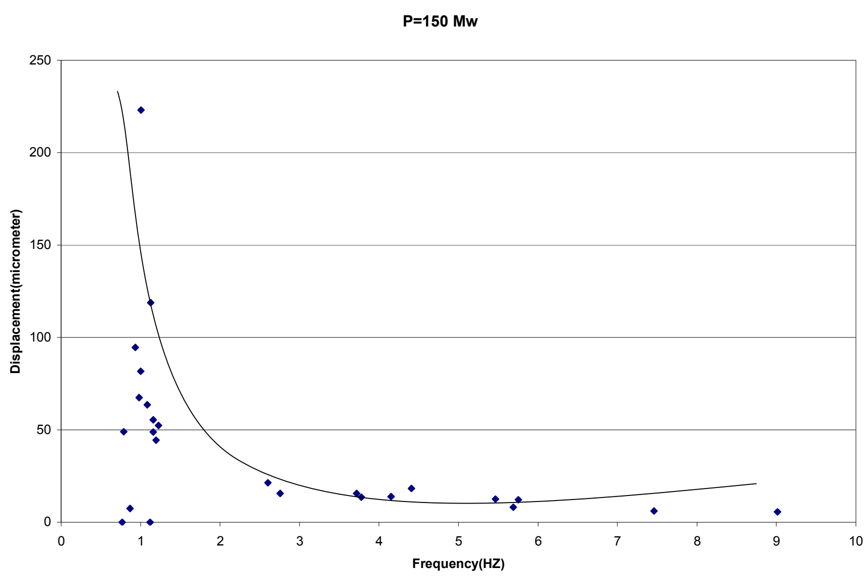

4.5 Cold Fusion Effects (cont'd)

- **B- Load Rejection - Jet Plasma**
  - **Impact on the runner and draft tube**
  - **Effects such as some cracks or pitting appear on the runner and draft tube**
  - **Pressure pulsation frequency**
  - **Hydrogen generation**

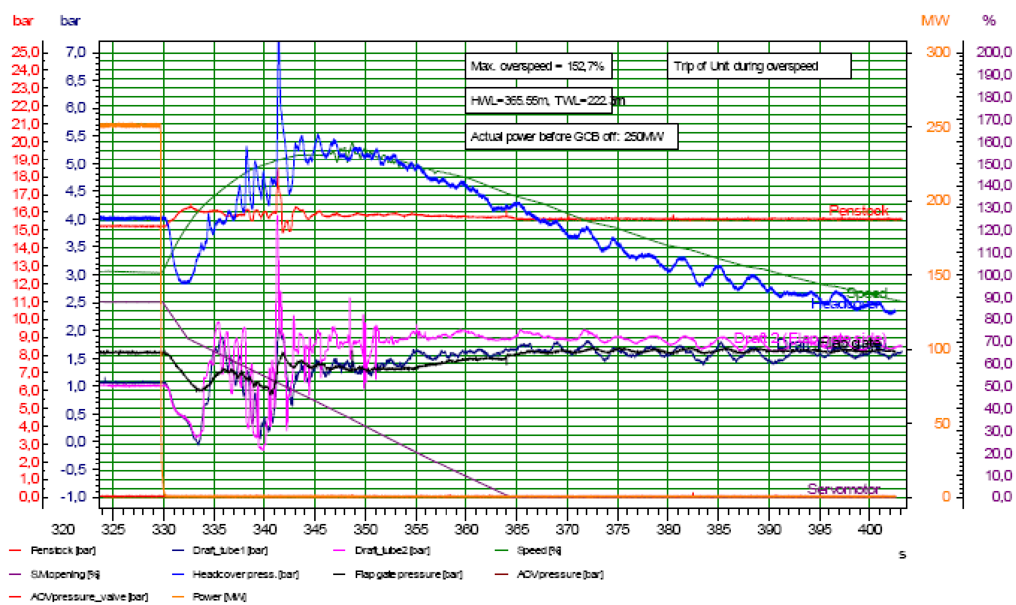

Crack on runner turbine

4.5 Cold Fusion Effects (cont'd)

- **C- Hydrogen Explosion**
  - CFD simulation of hydrogen explosion
  - The lift of rotating parts
  - The quantity of burnt hydrogen determine the volume of generating hydrogen

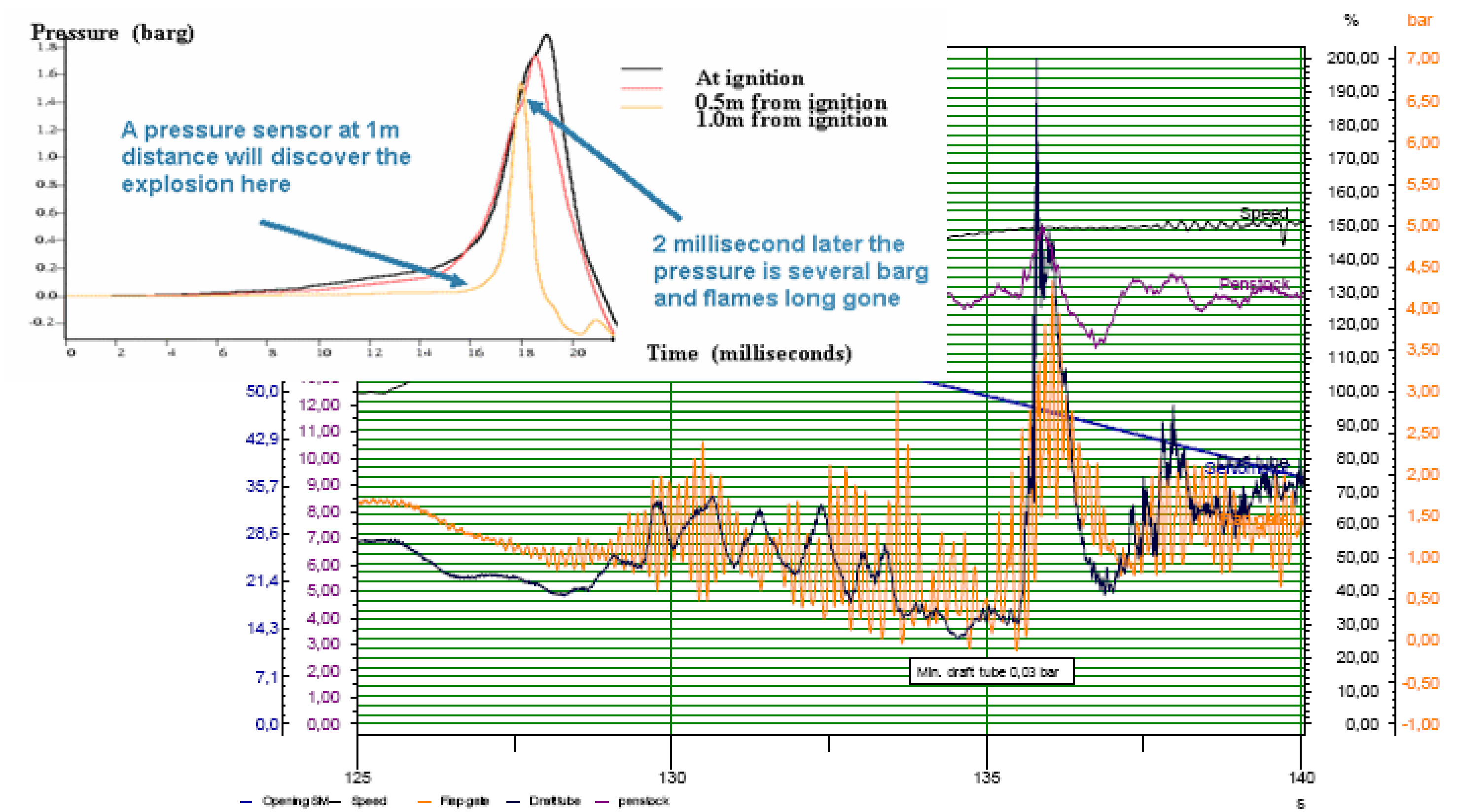

4.5 Cold Fusion Effects (cont'd)

- **D - Turbine Output**
  - **A new power is subtracted from the high and low pressure measuring sections**
  - A **balance of power allows the computation of the value of Em.**

$$E_m = E_{m2} - E_{m1} + \delta E_m$$

$$P_C = \rho Q[(e_1 - e_2) - E_m]$$

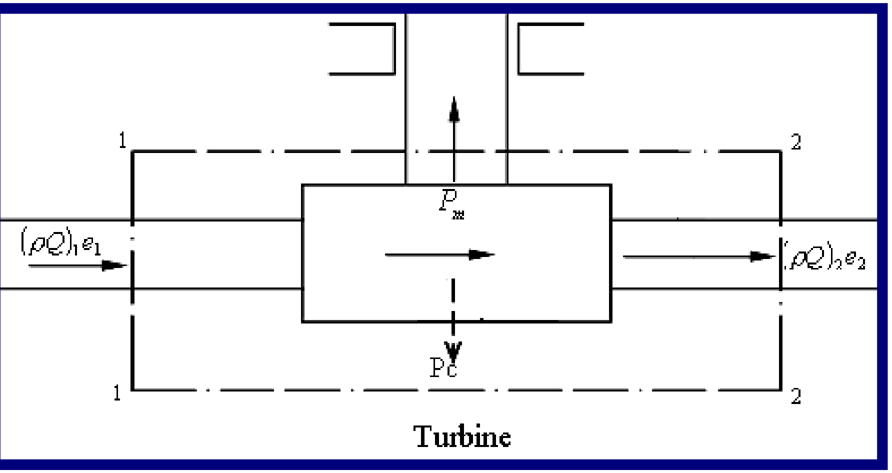

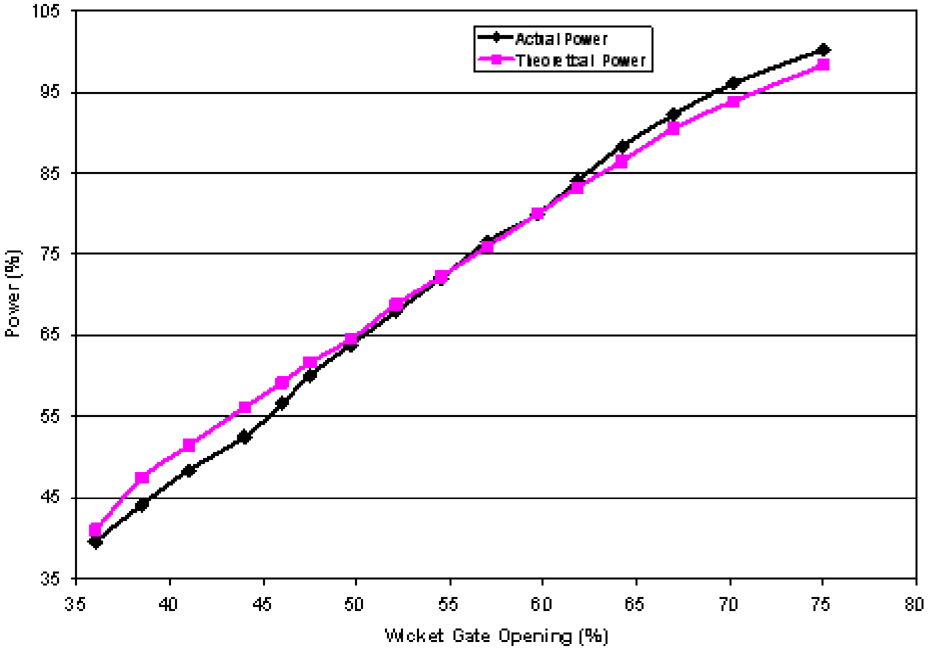

4.6 PAZ (Plasma Affected Zone)

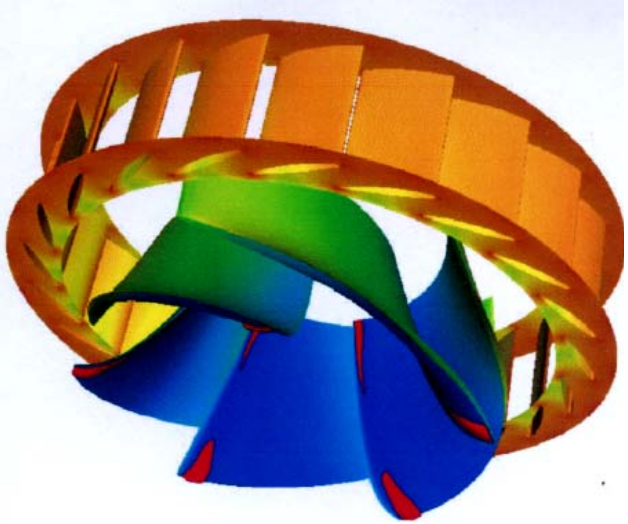

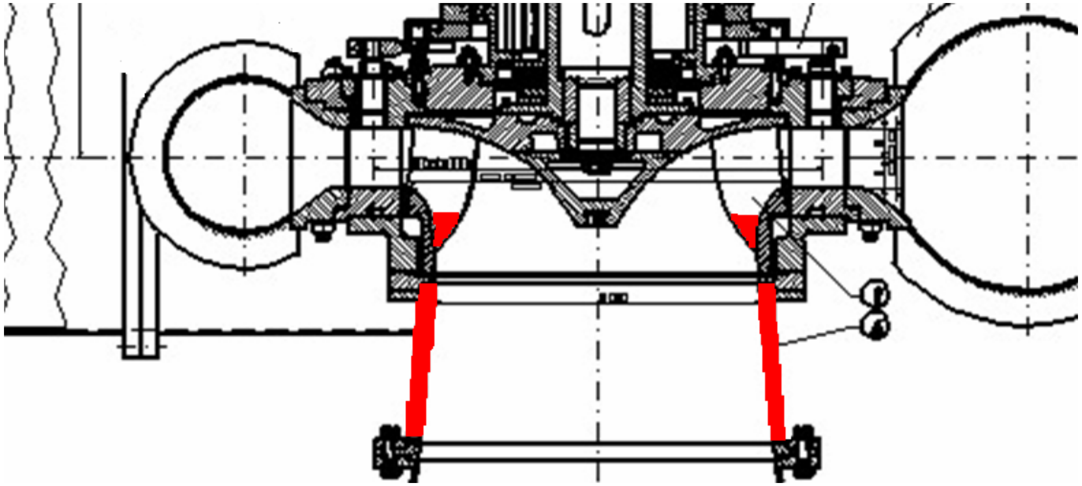

4.7 The Effects of Sigma and Reynolds

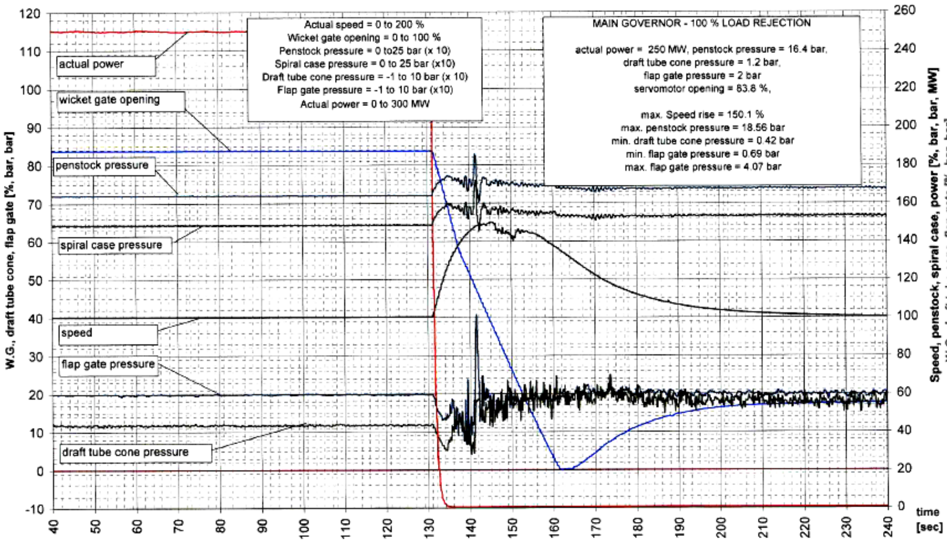

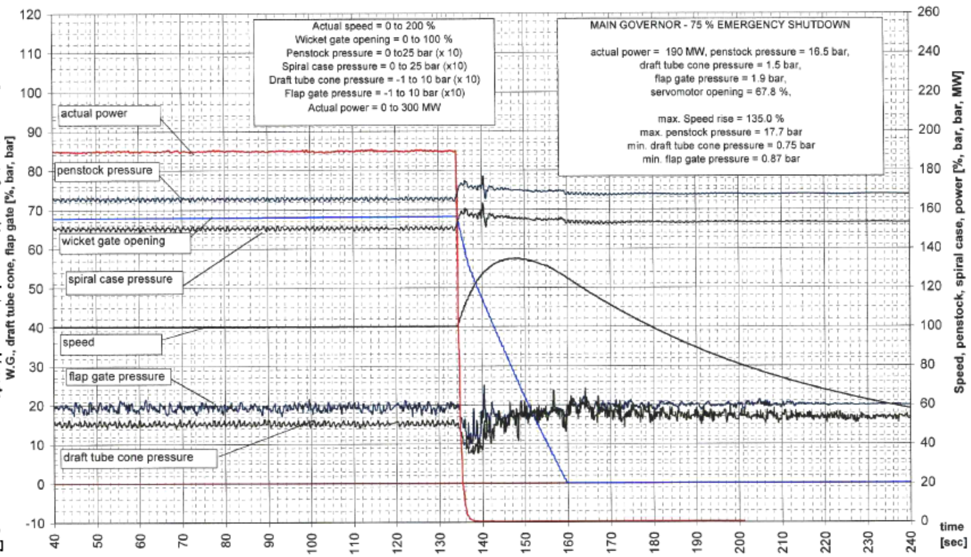

5 Conclusions

- There are main following notions, which can determine hydrogen and plasma process:
  - Luminescence
  - Turbine power effect
  - Shock pressure
  - Crack on turbine runner and daft tube
  - The lift of rotating parts
  - Impact effects
  - Noise
  - Hydrogen generation and explosion

- Hydro turbine can act as a reactor for cold fusion process